Transport Models for Seismic Scattering

Second SPIN Workshop, Carcans, France

L. Margerin,
S. Menina, N. Compaire, M. Celorio, A. Barajas, A. Delsuc, J. Marti,
R. Garcia, M. Calvet, E. Chaljub, M. Campillo, T. Kawamura P. Lognonné, …

irap
astrophysique & planétologie

Planetary Seismology: a variety of propagation regimes

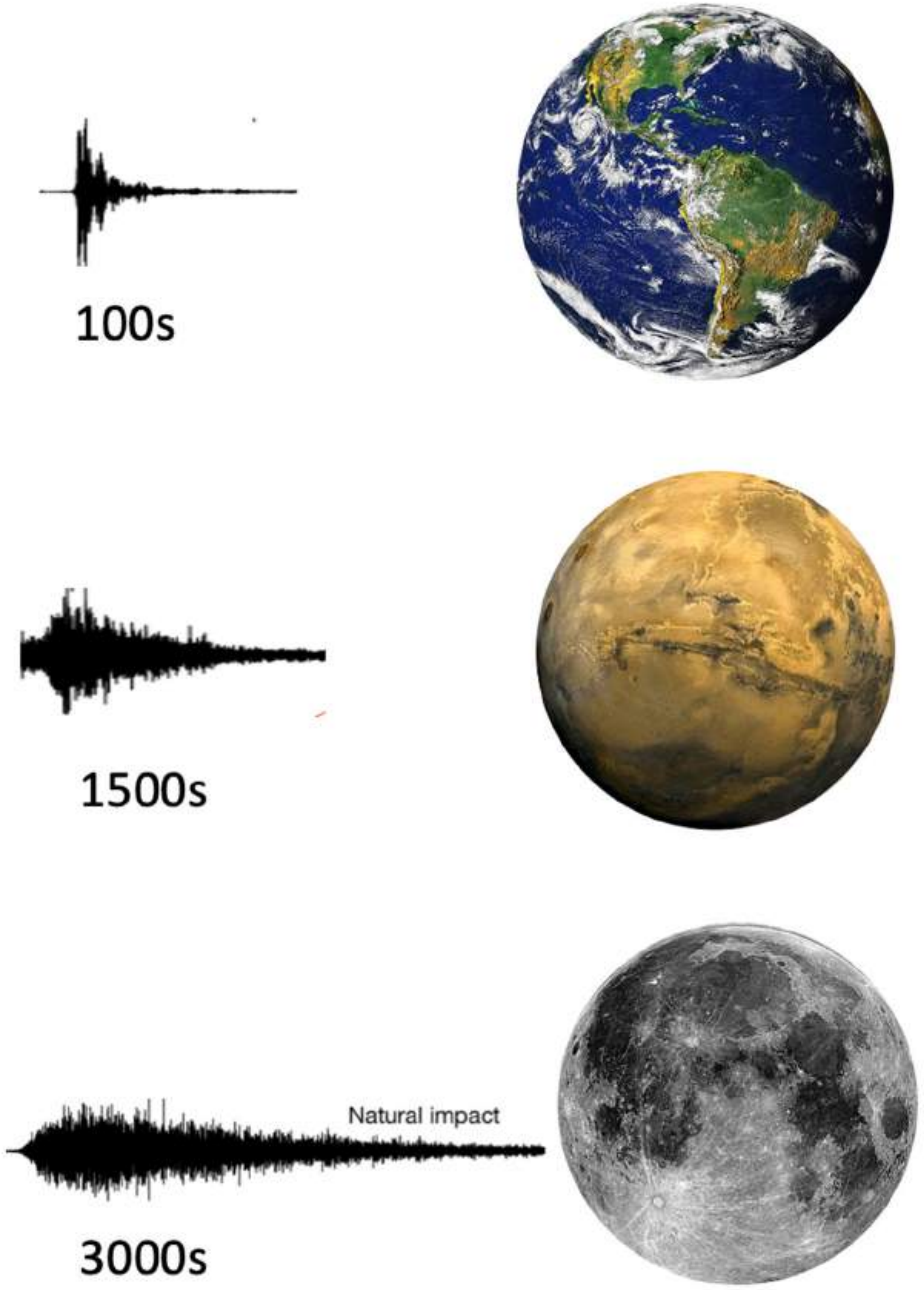

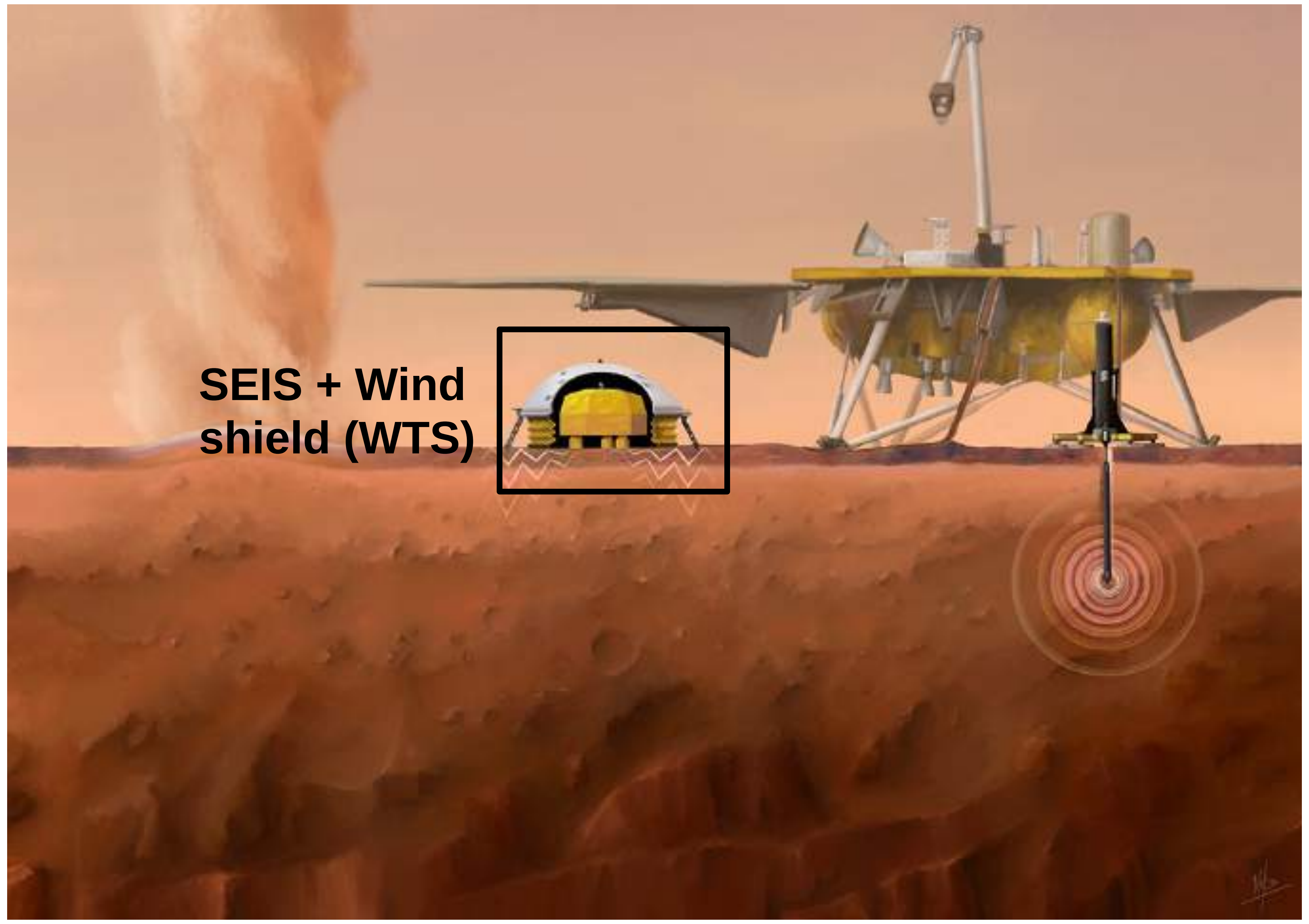

Seismic Attenuation

Attenuation Q^{-1} = Scattering Q_{sc}^{-1} + Absorption Q_i^{-1}

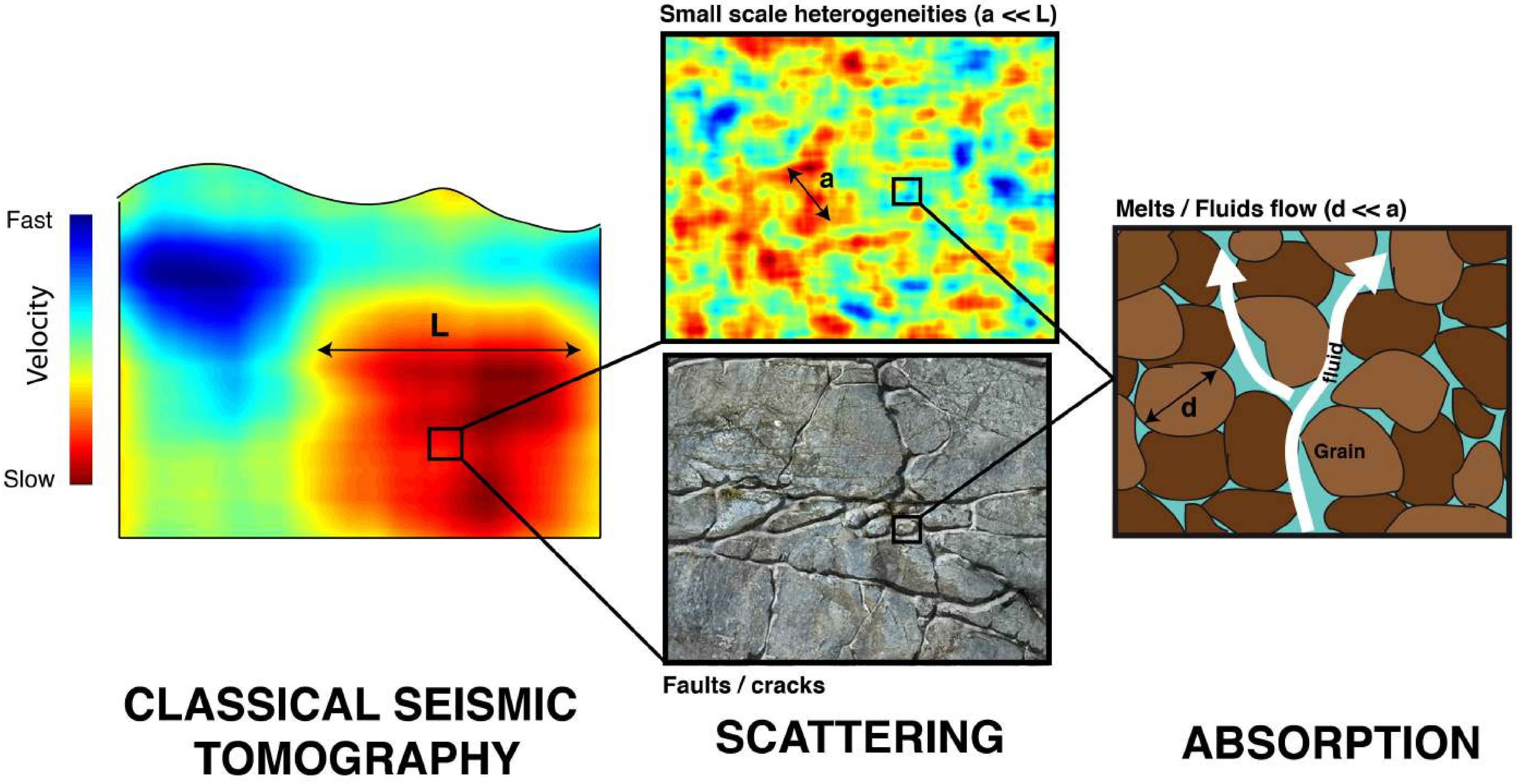

Heterogeneity

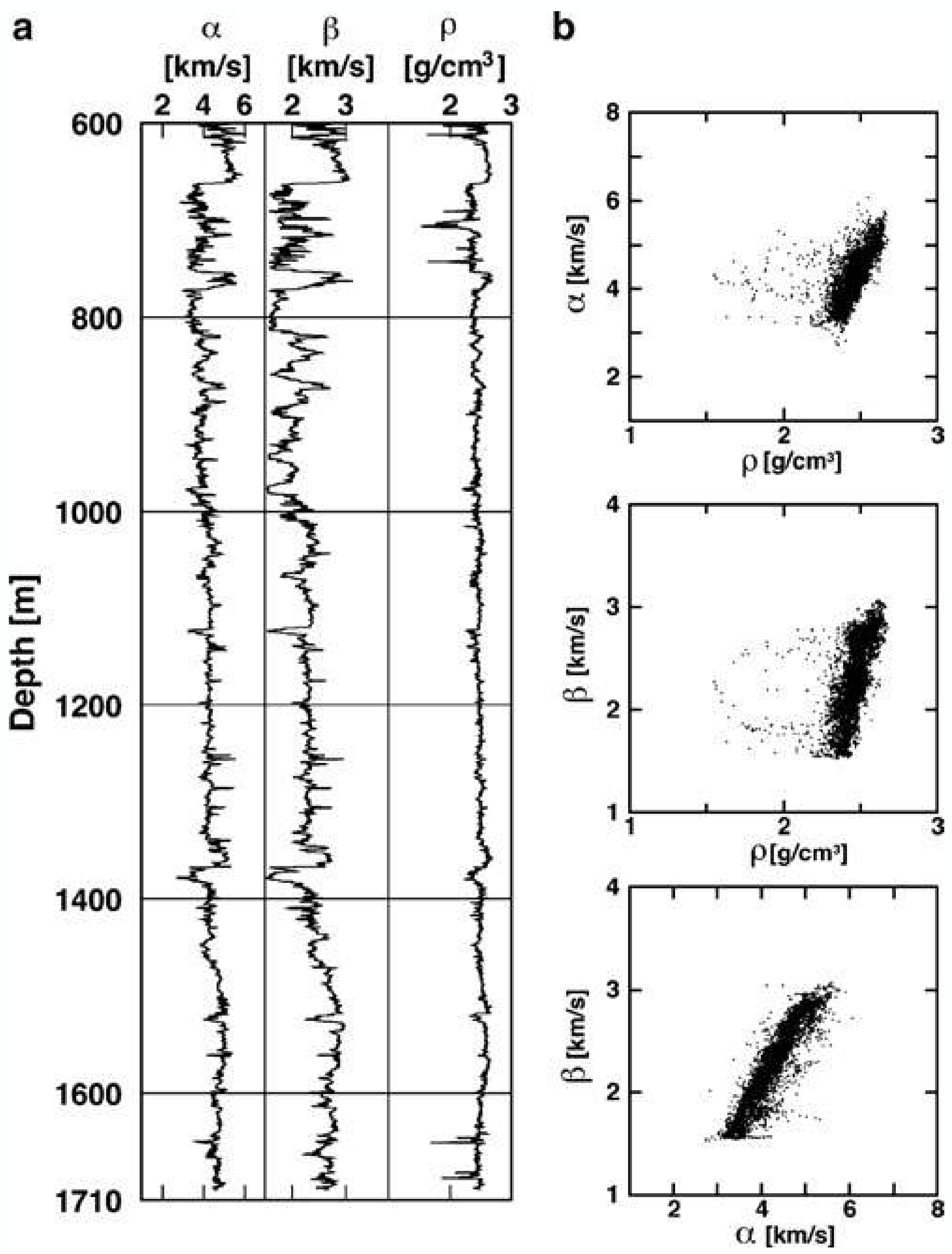

Shiomi 1997

Correlation Function

$$C(\boldsymbol{r}) = \frac{1}{\langle v \rangle^2} \langle \delta v(\mathbf{x} + \boldsymbol{r}/2) \delta v(\mathbf{x} - \boldsymbol{r}/2) \rangle$$

$$\frac{\delta \rho}{\rho} = \nu \frac{\delta v}{v}$$ ← Birch Law

Heterogeneity

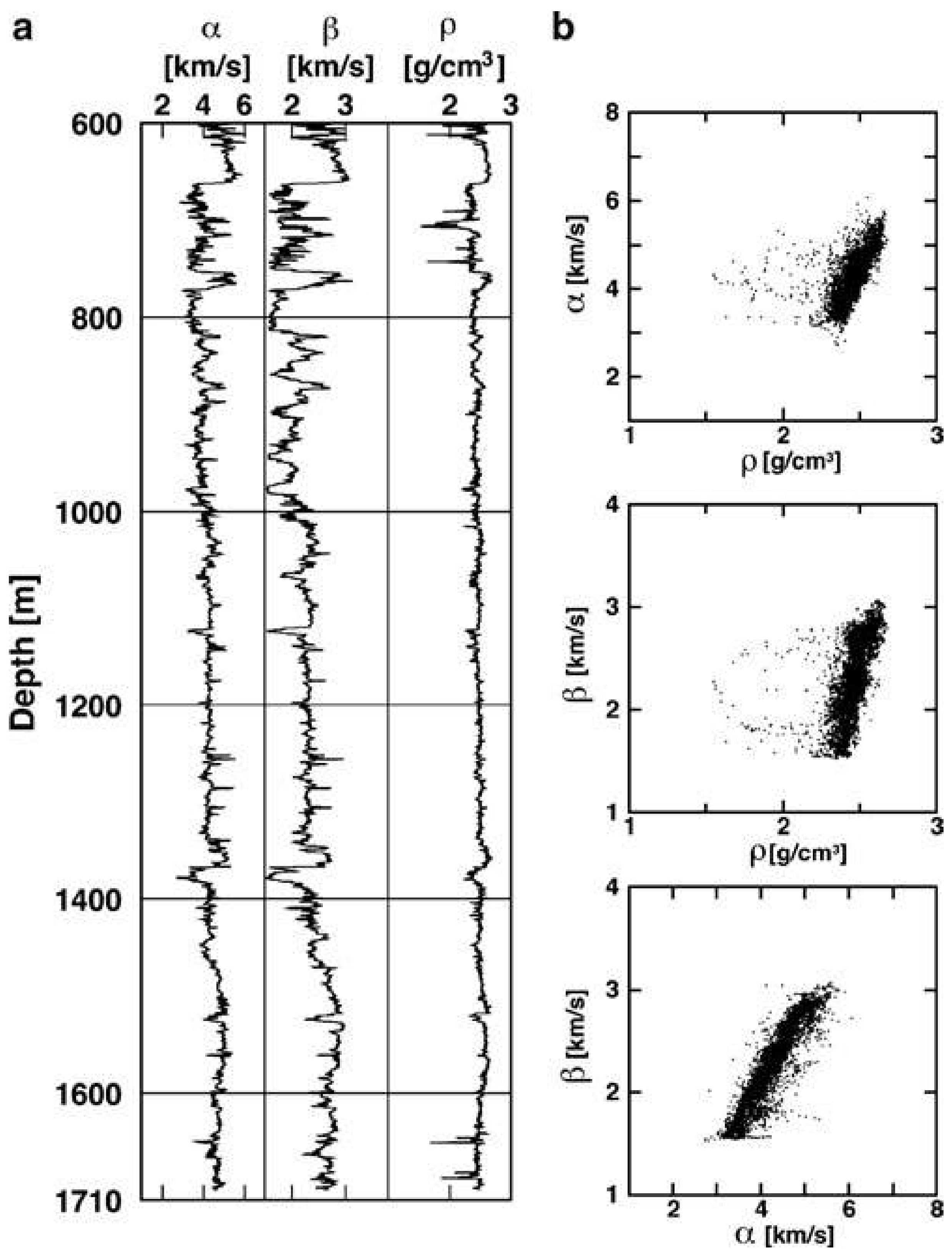

Shiomi 1997

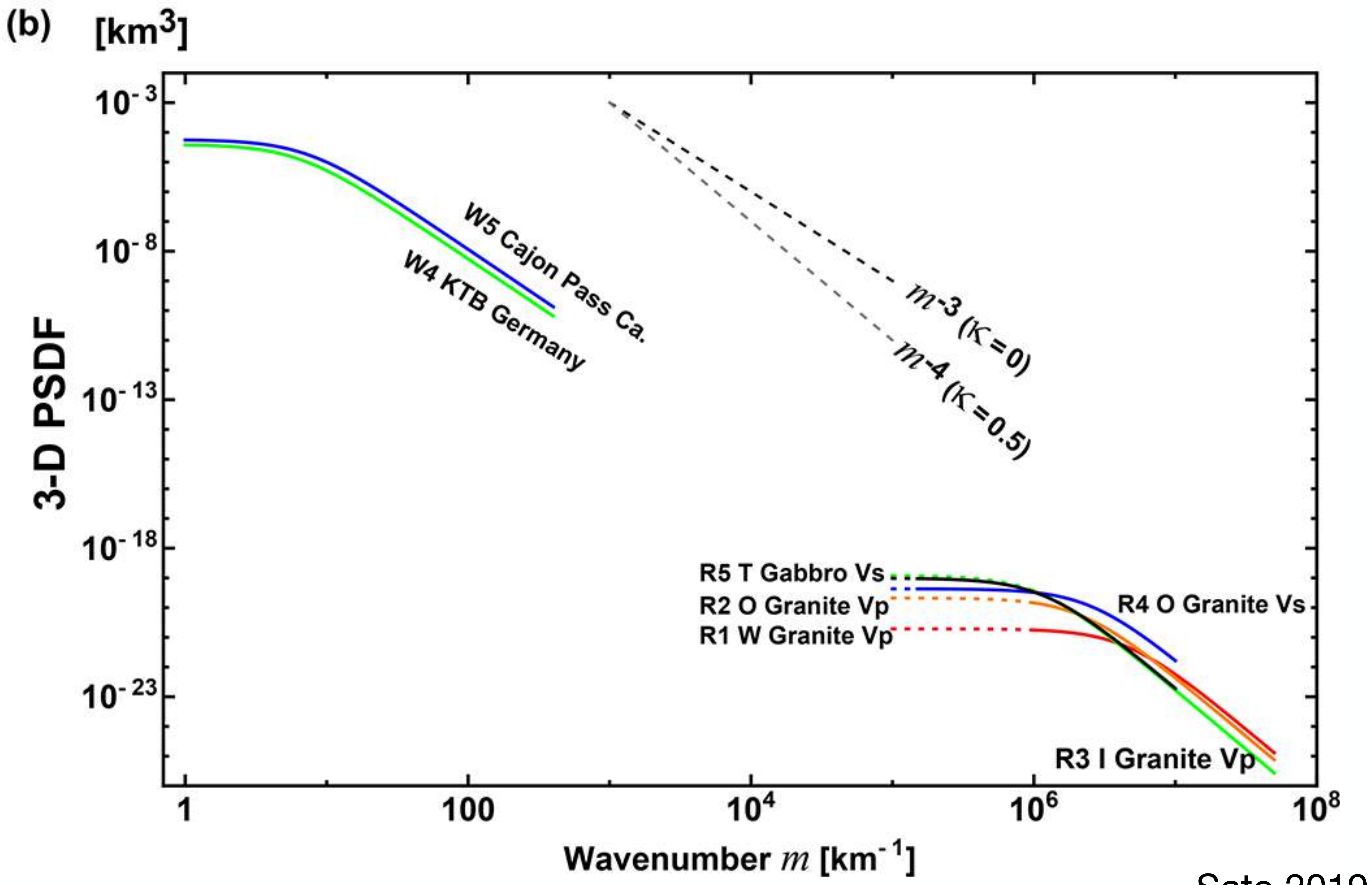

Sato 2019

Correlation Function

$$C(\boldsymbol{r}) = \frac{1}{\langle v\rangle^2}\langle \delta v(\mathbf{x}+\boldsymbol{r}/2)\delta v(\mathbf{x}-\boldsymbol{r}/2)\rangle$$

$$\frac{\delta\rho}{\rho} = \nu\frac{\delta v}{v}$$

← Birch Law

Power Spectrum

$$\Phi(\boldsymbol{m}) = \int_{\mathbb{R}^3} C(\boldsymbol{r})\, e^{i\boldsymbol{m}\cdot\boldsymbol{r}}\, d\boldsymbol{r}$$

$$\propto \frac{\epsilon^2 a^3}{(1+m^2a^2)^{\kappa+3/2}}$$

Hurst Exponent

Heterogeneity

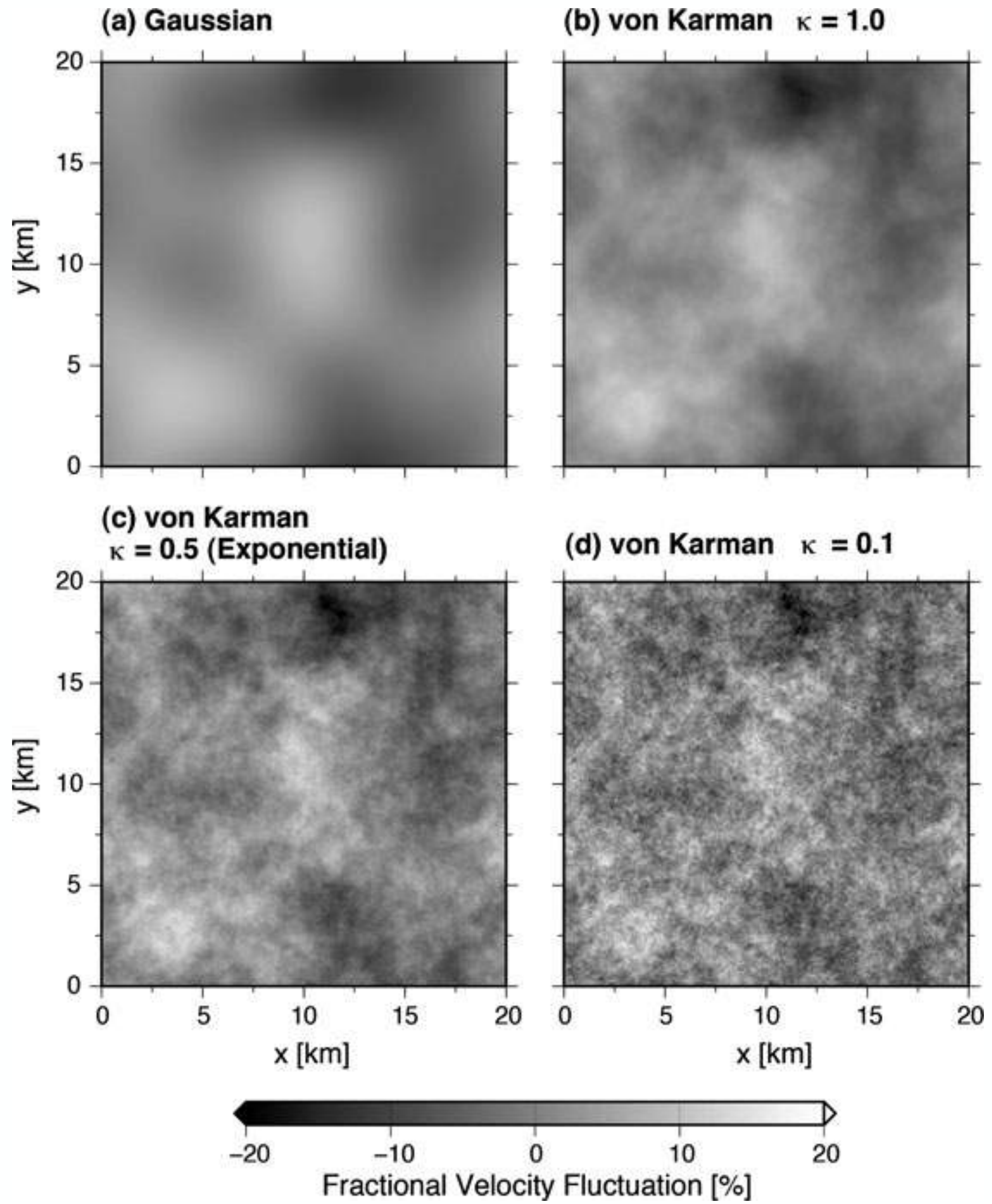

Sato et al, 2012

Multiple Scattering

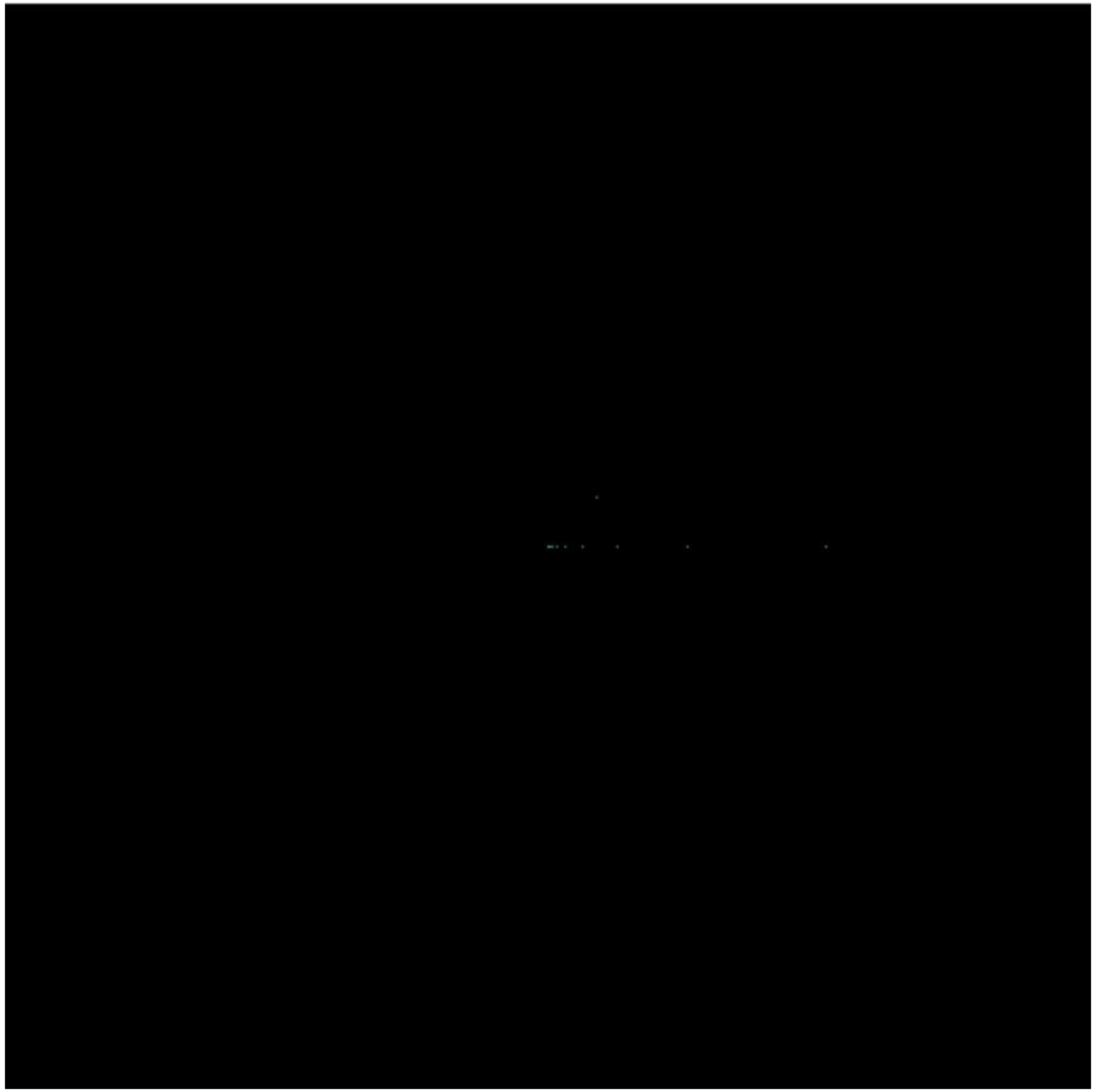

- 2-D anti-plane geometry (SH)
- Slab of random material with exponential correlation
- Correlated fluctuations of density and velocity
- Periodic Boundary Conditions on the sides
- Absorbing Boundary Conditions at Top and Bottom
- Numerical Solution with SpecFem2D

Celorio et al., in prep.

Coherent Field

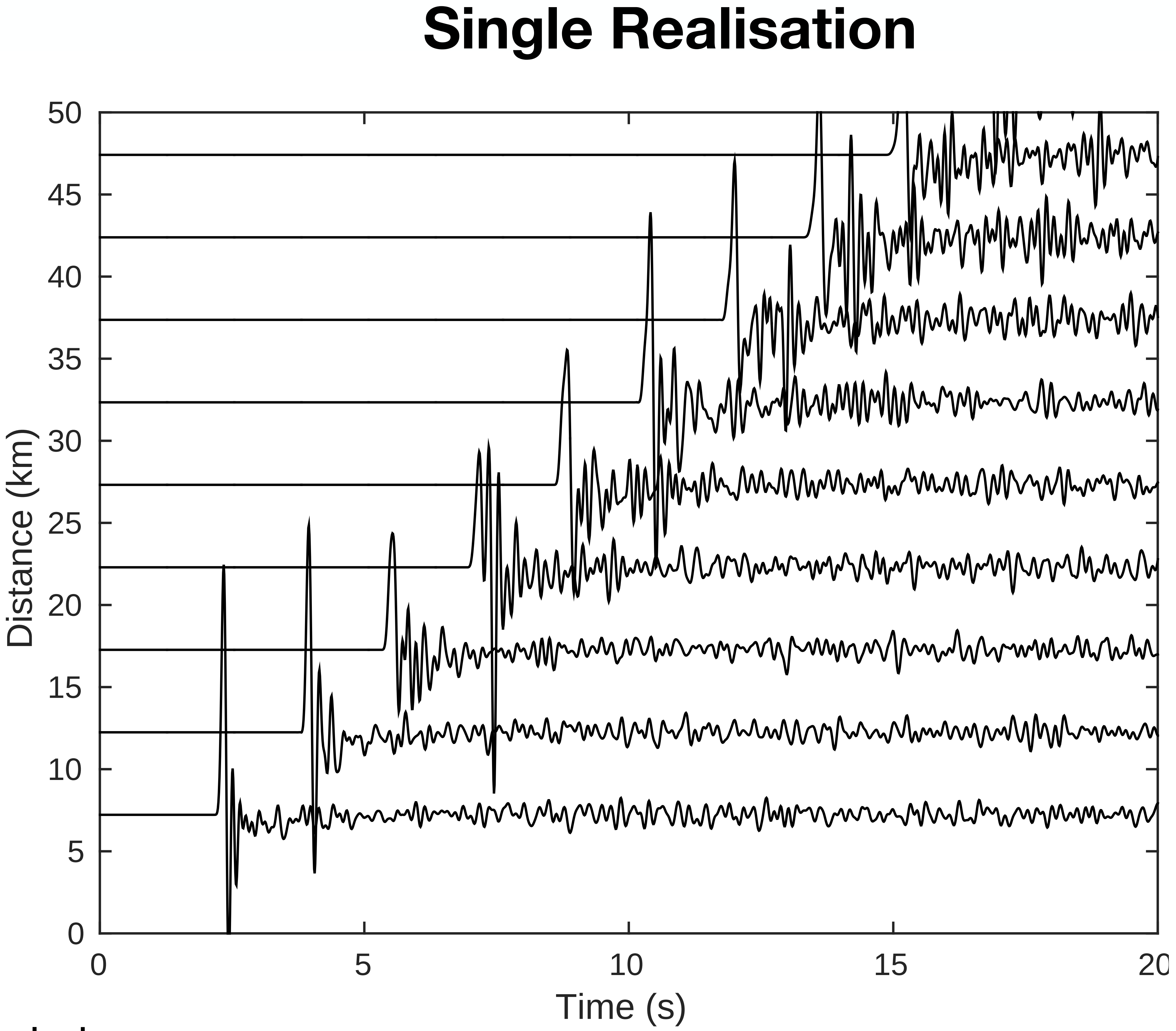

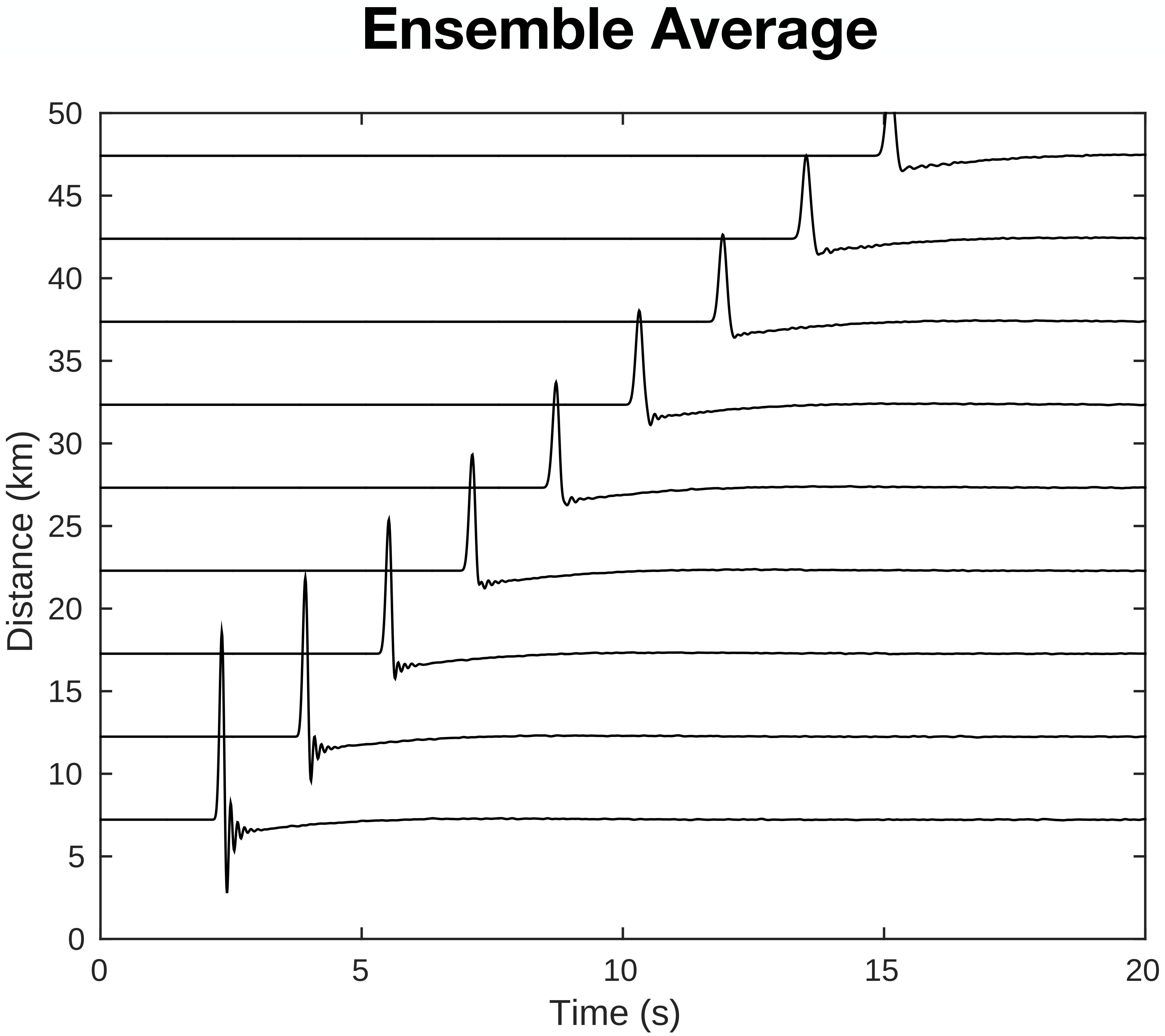

Celorio et al., in prep.

$\langle u \rangle \propto e^{-r/l}$ l : scattering mean free path

Frequency Regimes

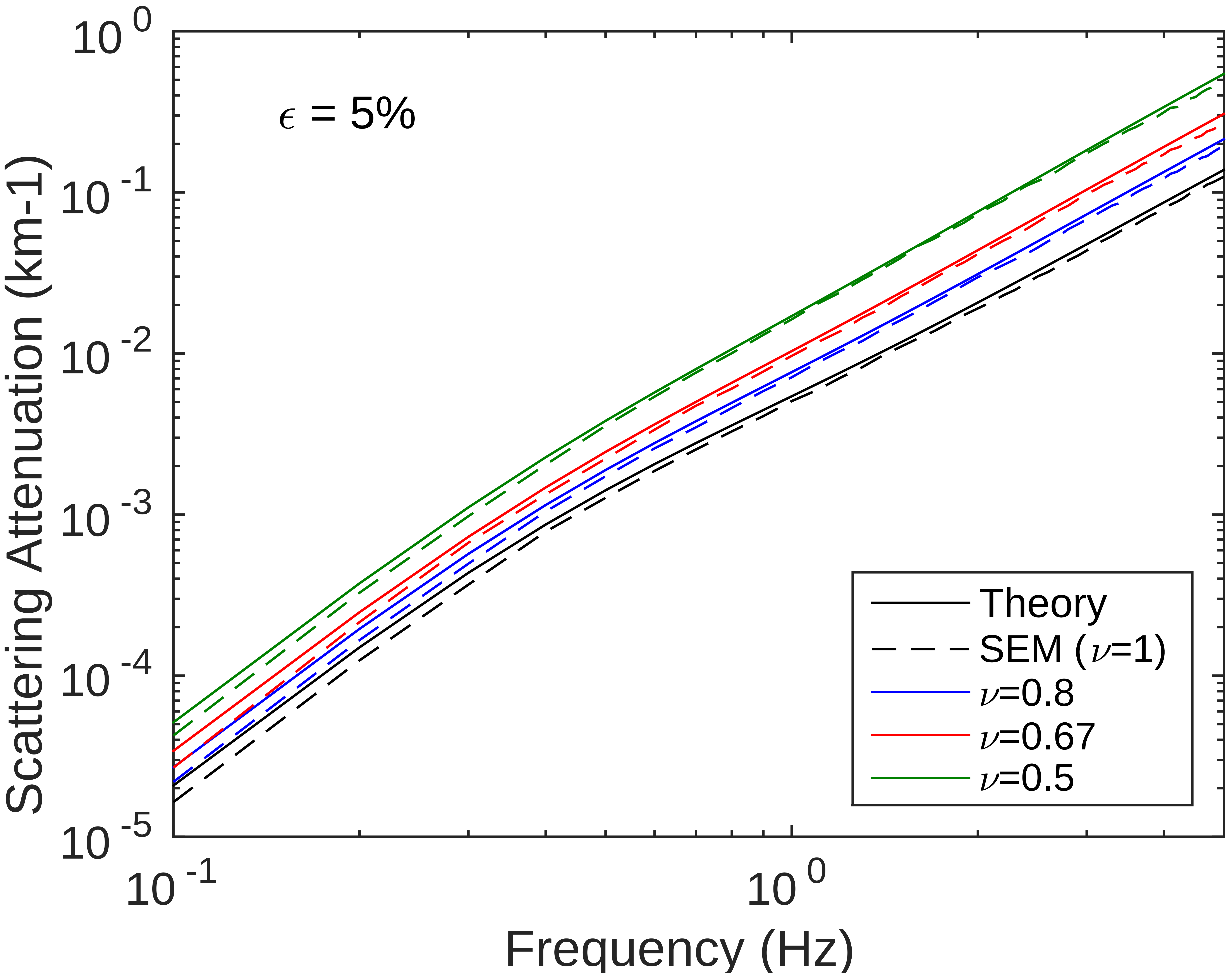

Celorio et al., in prep.

Frequency Regimes

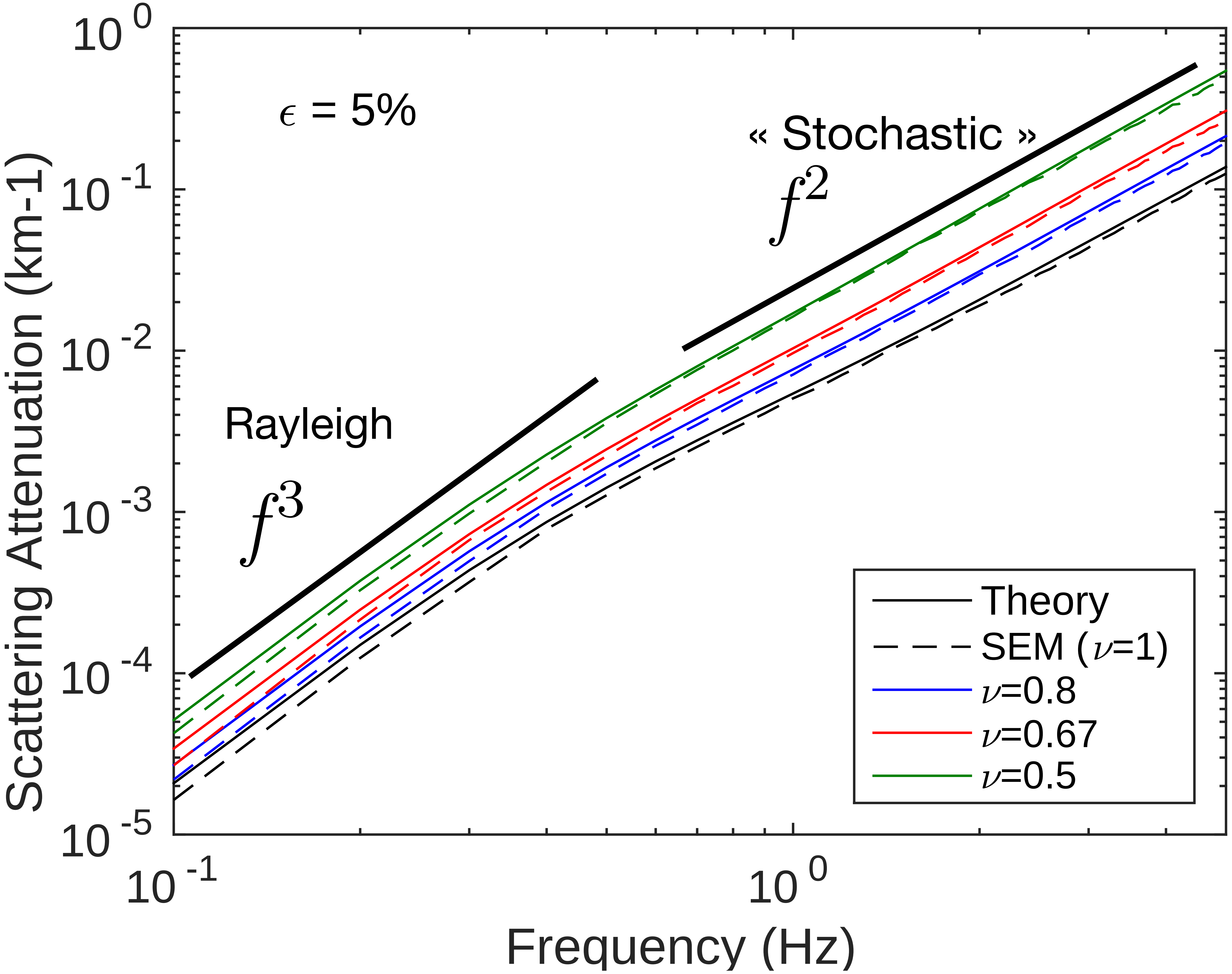

Celorio et al., in prep.

Frequency Regimes

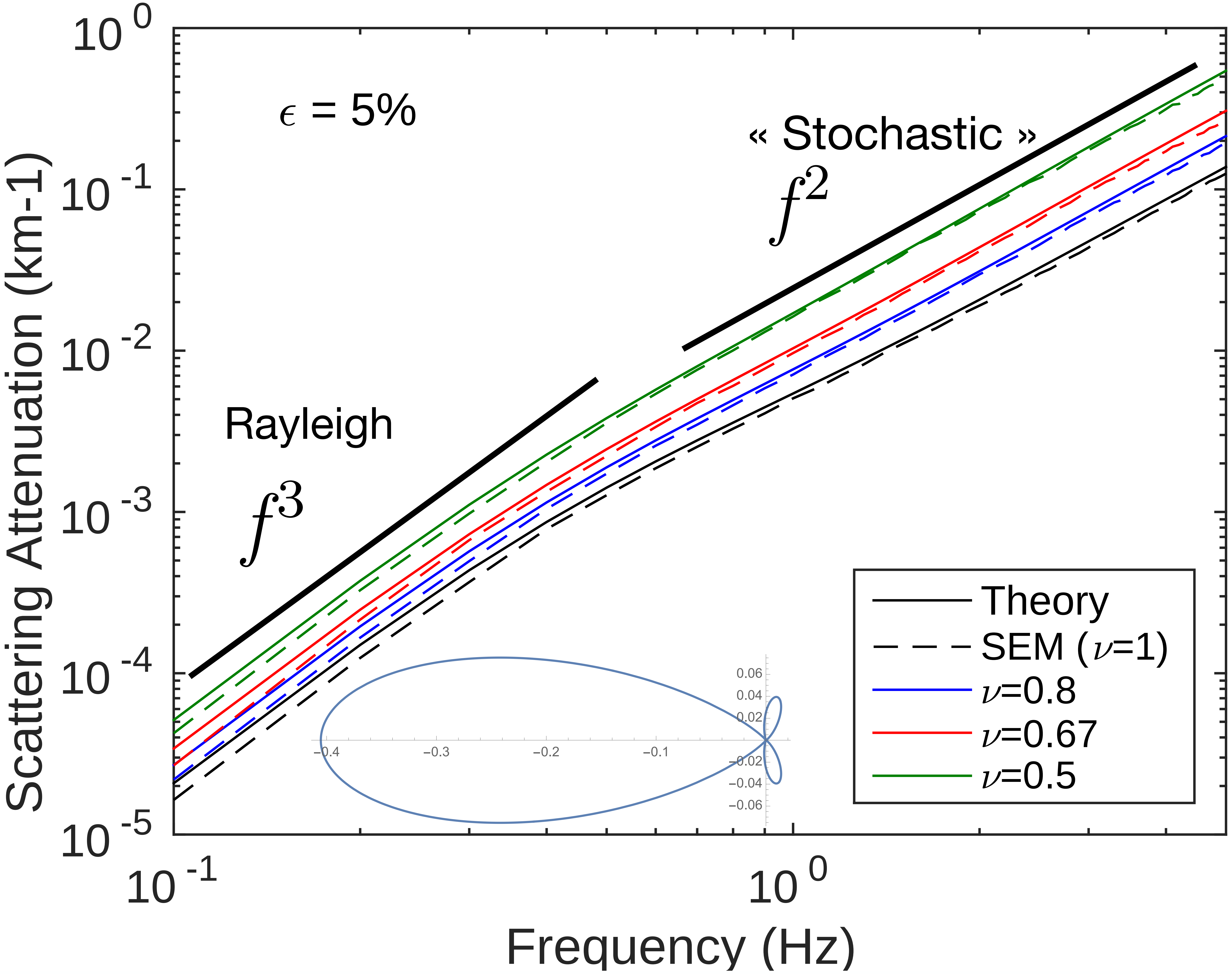

Scattering Anisotropy

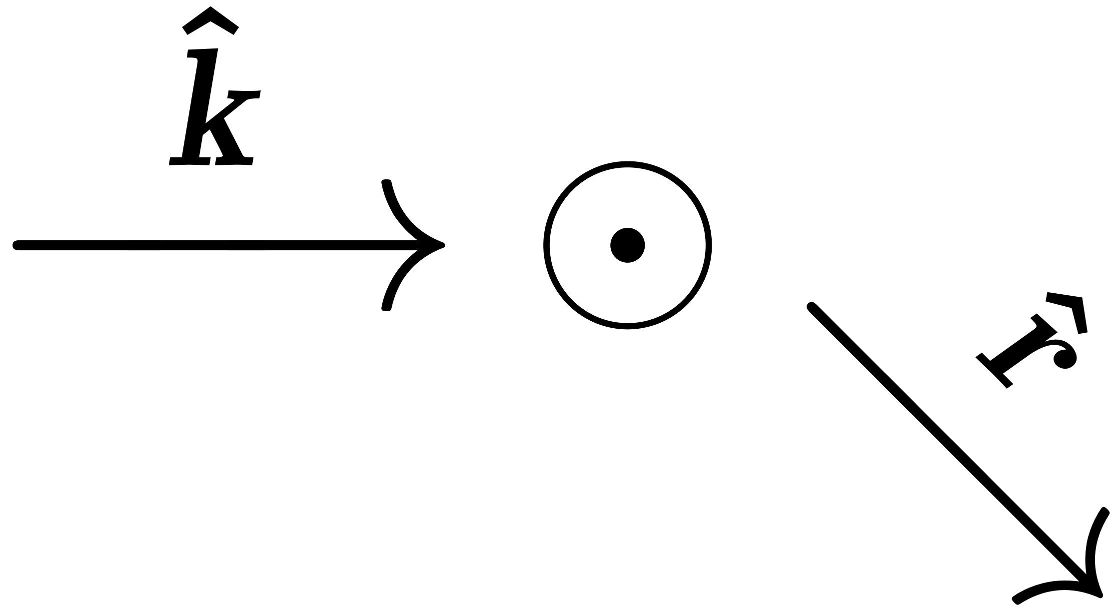

Rayleigh Regime

$$p(\hat{\boldsymbol{k}}, \hat{\mathbf{r}}) = F\left(\delta(\rho c), \delta c, \hat{\boldsymbol{k}} \cdot \hat{\mathbf{r}}\right)$$

↑

Impedance Fluctuations

Celorio et al., in prep.

Frequency Regimes

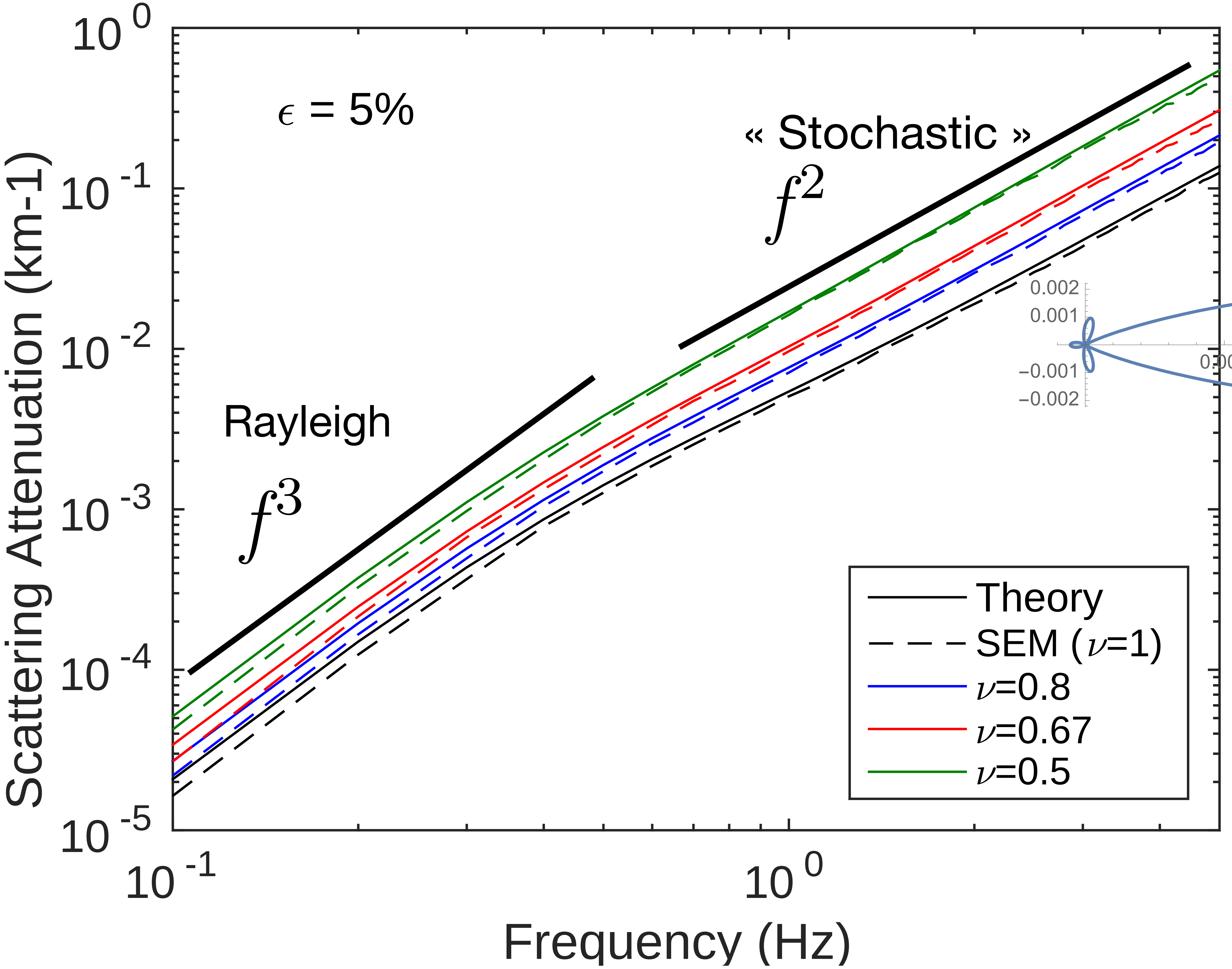

Scattering Anisotropy

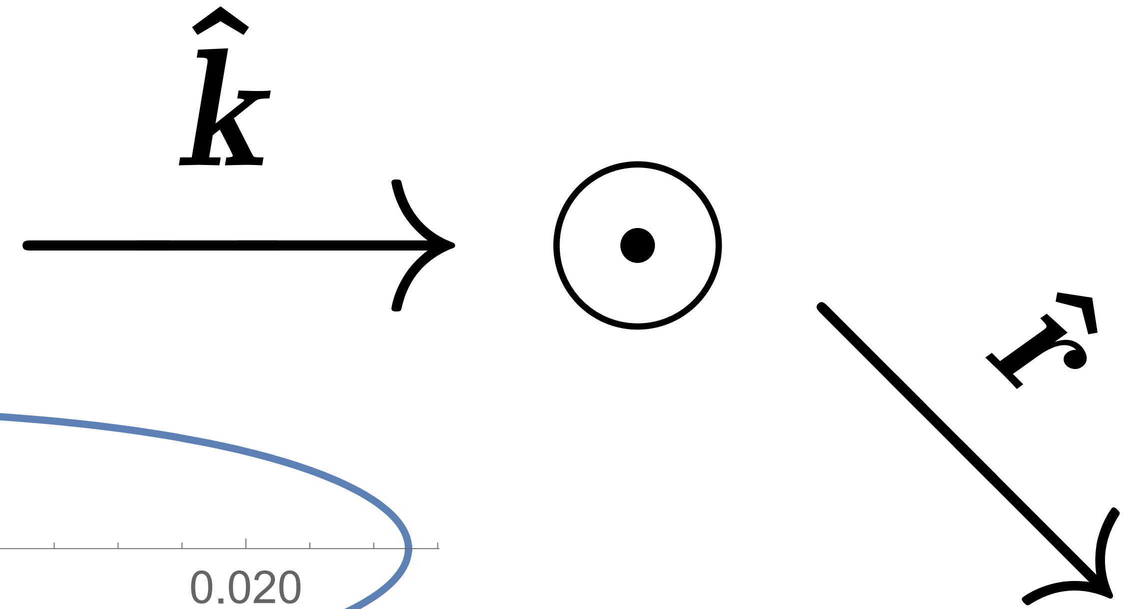

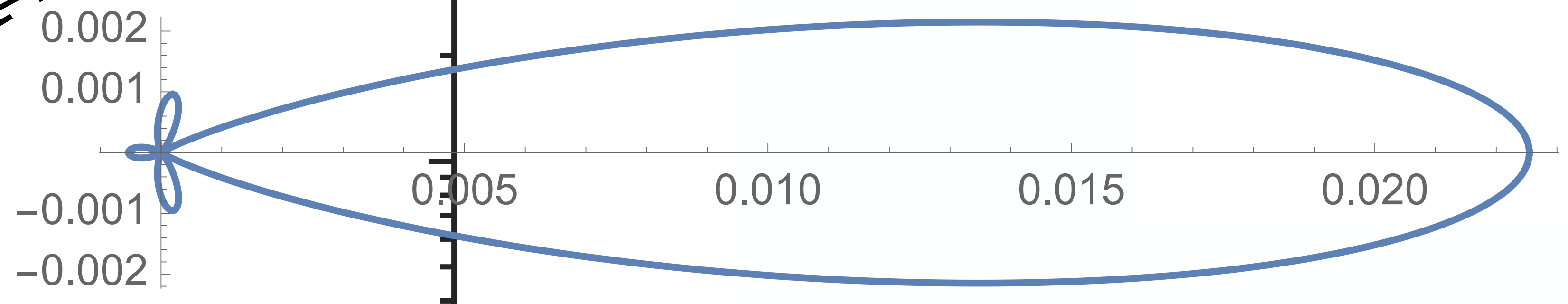

Stochastic Regime

$$p(\hat{\mathbf{k}},\hat{\mathbf{r}}) = F\left(\delta(\rho c), \delta c, \hat{\mathbf{k}}\cdot\hat{\mathbf{r}}\right)\boxed{\Phi(\hat{\mathbf{k}}-\hat{\mathbf{r}})}$$

Power Spectrum of Fluctuations

Celorio et al., in prep.

Mean Intensity $I = \langle u^2 \rangle$

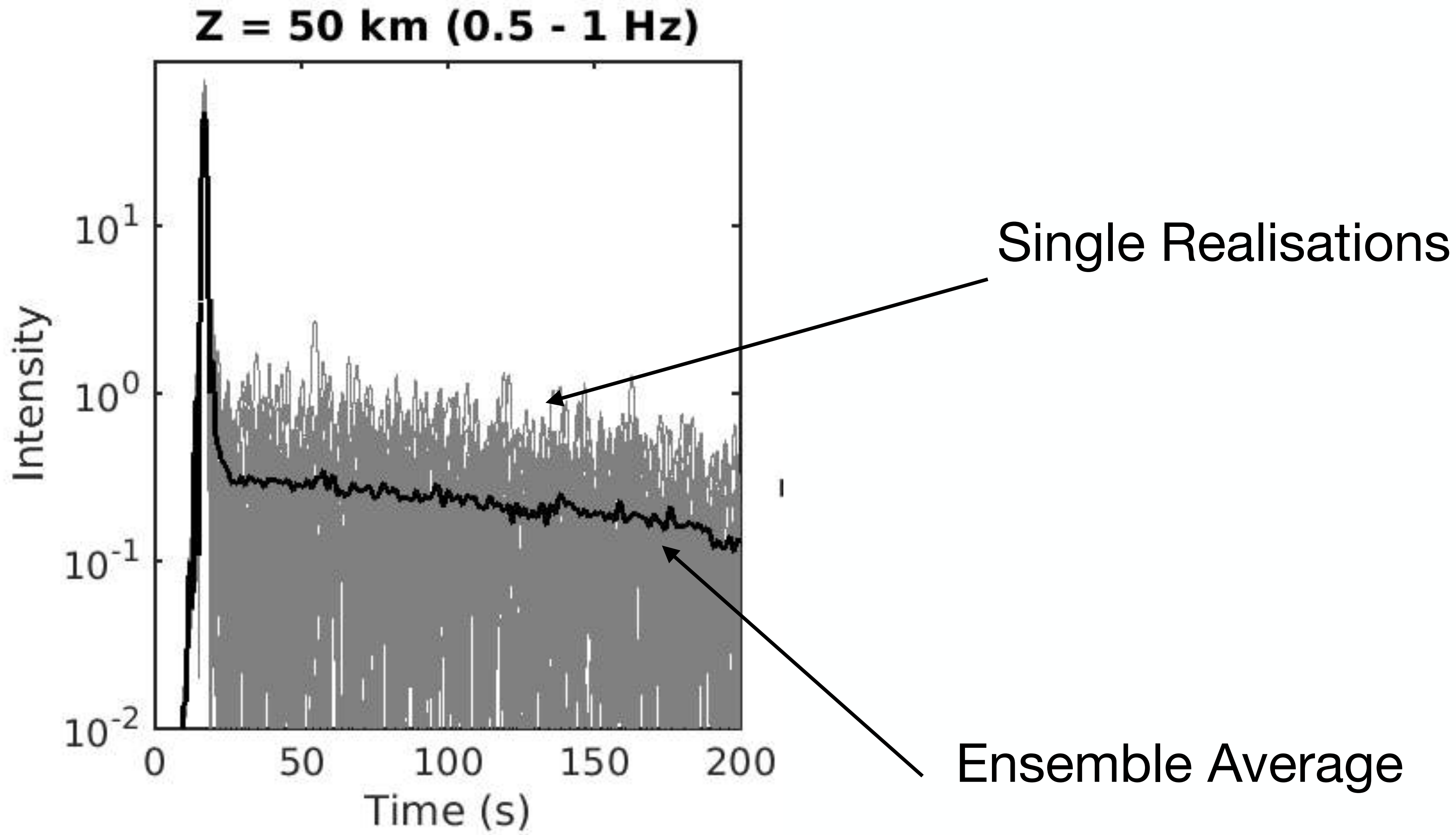

Mean Intensity $I = \langle u^2 \rangle$

$$\overbrace{\left(\frac{\partial}{\partial t} + c\widehat{\mathbf{k}}\cdot\nabla_{\mathbf{X}} + \omega(Q_{sc}^{-1}+Q_i^{-1})\right)}^{\text{Coherent Propagation}} I(\mathbf{X},\widehat{\mathbf{k}},t) =$$

$$Q_{sc} = \frac{\omega l}{c}$$

$$Q_i = \frac{\omega l_a}{c}$$

$$\overbrace{\omega Q_{sc}^{-1}\oint \overbrace{p(\widehat{\mathbf{k}},\widehat{\mathbf{k}}')}^{\text{Scattering anisotropy}} I(\mathbf{X},\widehat{\mathbf{k}}',t)\,d^2\hat{k}'}^{\text{Multiple Scattering Term}} + \overbrace{S(\mathbf{X},\widehat{\mathbf{k}},t)}^{\text{Source term}}$$

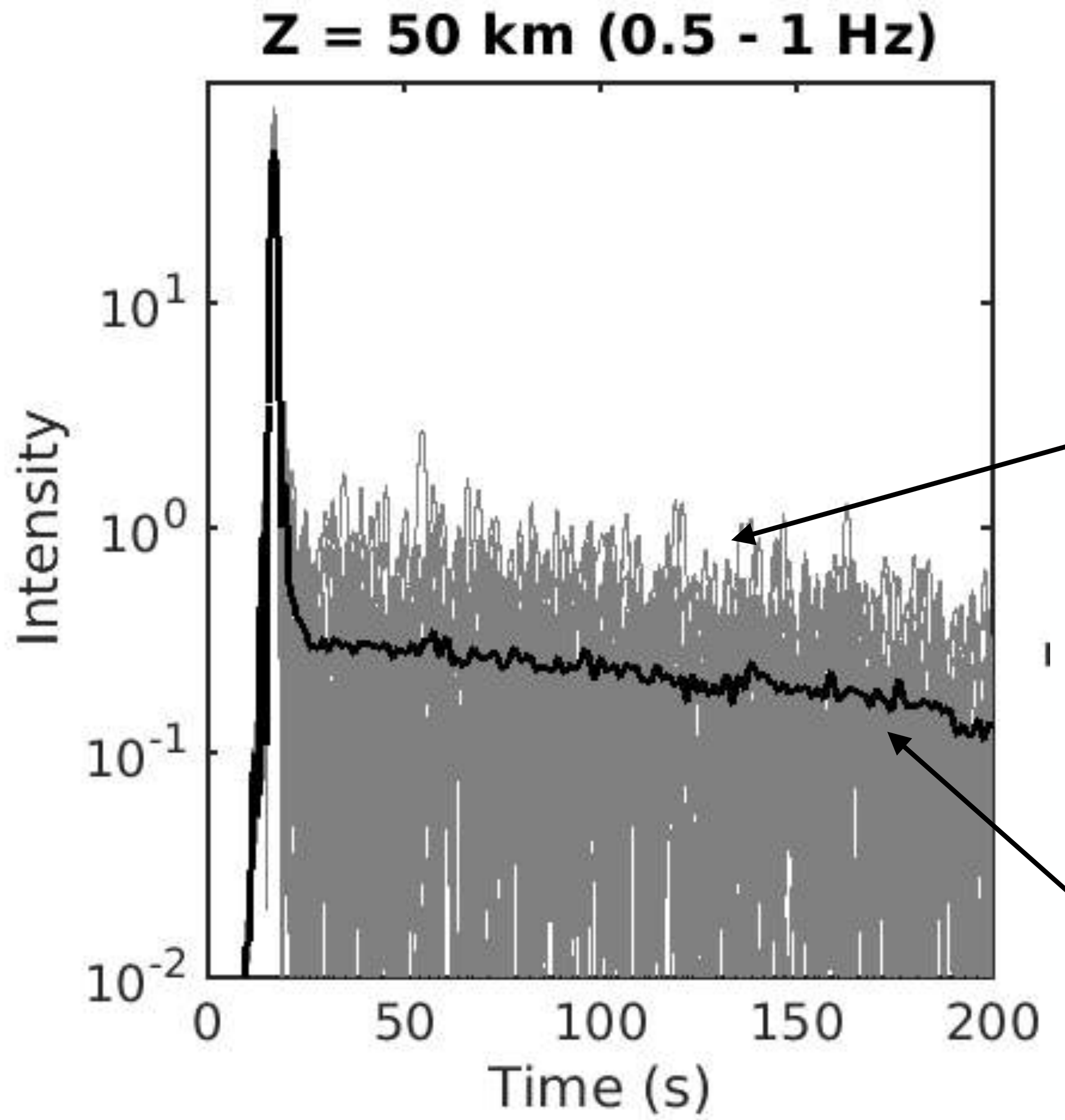

Single Realisations

Ensemble Average

« Specific Intensity »

=

Angularly Resolved Energy Flux

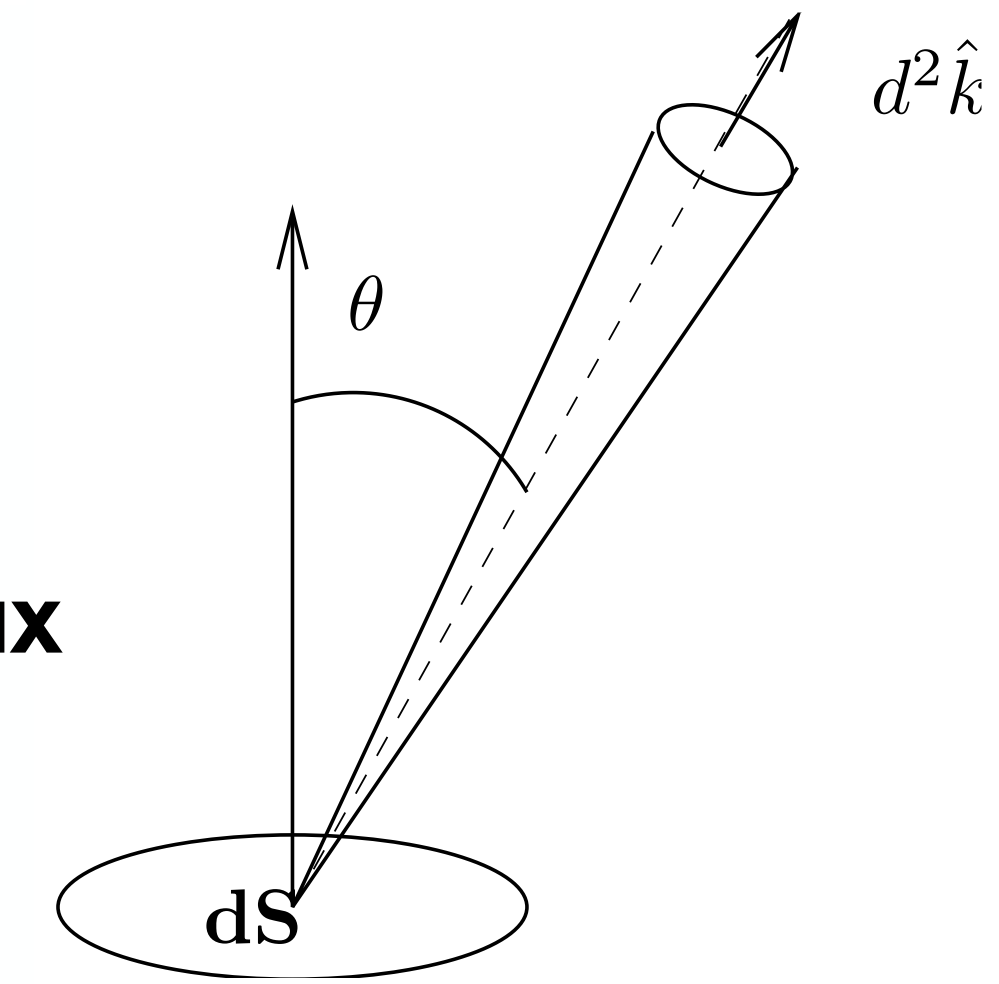

Mean Intensity $\quad I = \langle u^2 \rangle$

$$\overbrace{\left(\frac{\partial}{\partial t} + c\widehat{\mathbf{k}}\cdot\nabla_{\mathbf{X}} + \omega(Q_{sc}^{-1} + Q_i^{-1})\right)}^{\text{Coherent Propagation}} I(\mathbf{X},\widehat{\mathbf{k}},t) =$$

$$Q_{sc} = \frac{\omega l}{c}$$

$$Q_i = \frac{\omega l_a}{c}$$

$$\overbrace{\omega Q_{sc}^{-1} \oint \overbrace{p(\widehat{\mathbf{k}},\widehat{\mathbf{k}}')}^{\text{Scattering anisotropy}} I(\mathbf{X},\widehat{\mathbf{k}}',t)\, d^2\hat{k}'}^{\text{Multiple Scattering Term}} + \overbrace{S(\mathbf{X},\widehat{\mathbf{k}},t)}^{\text{Source term}}$$

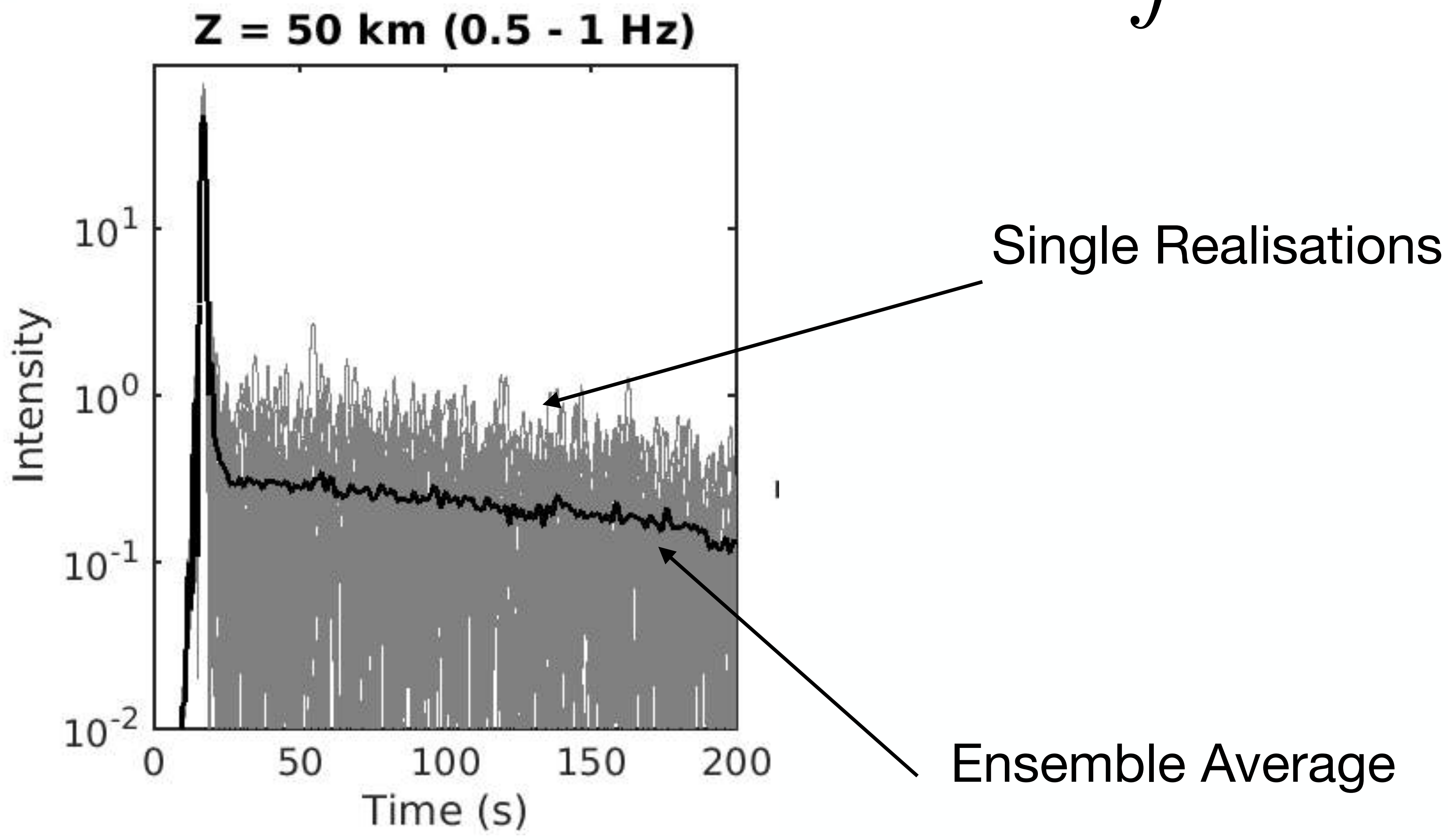

SEM / Radiative Transfer

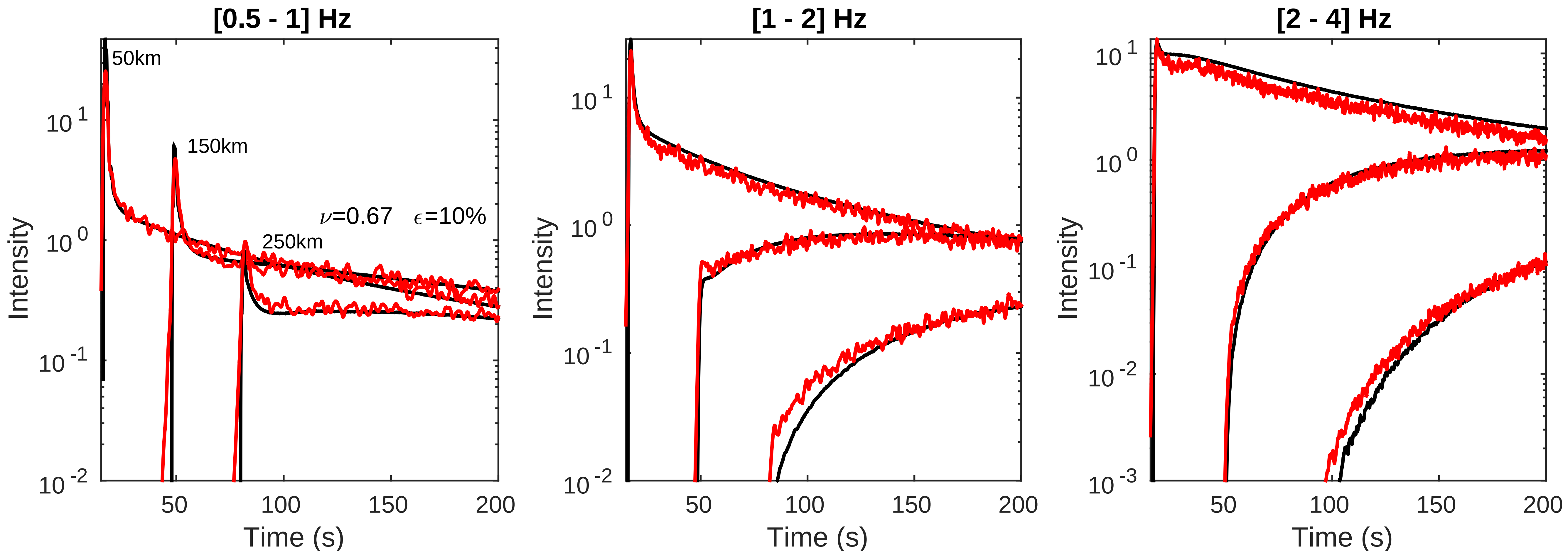

Separation of Scattering and Absorption

Different scaling for coherent and incoherent intensity

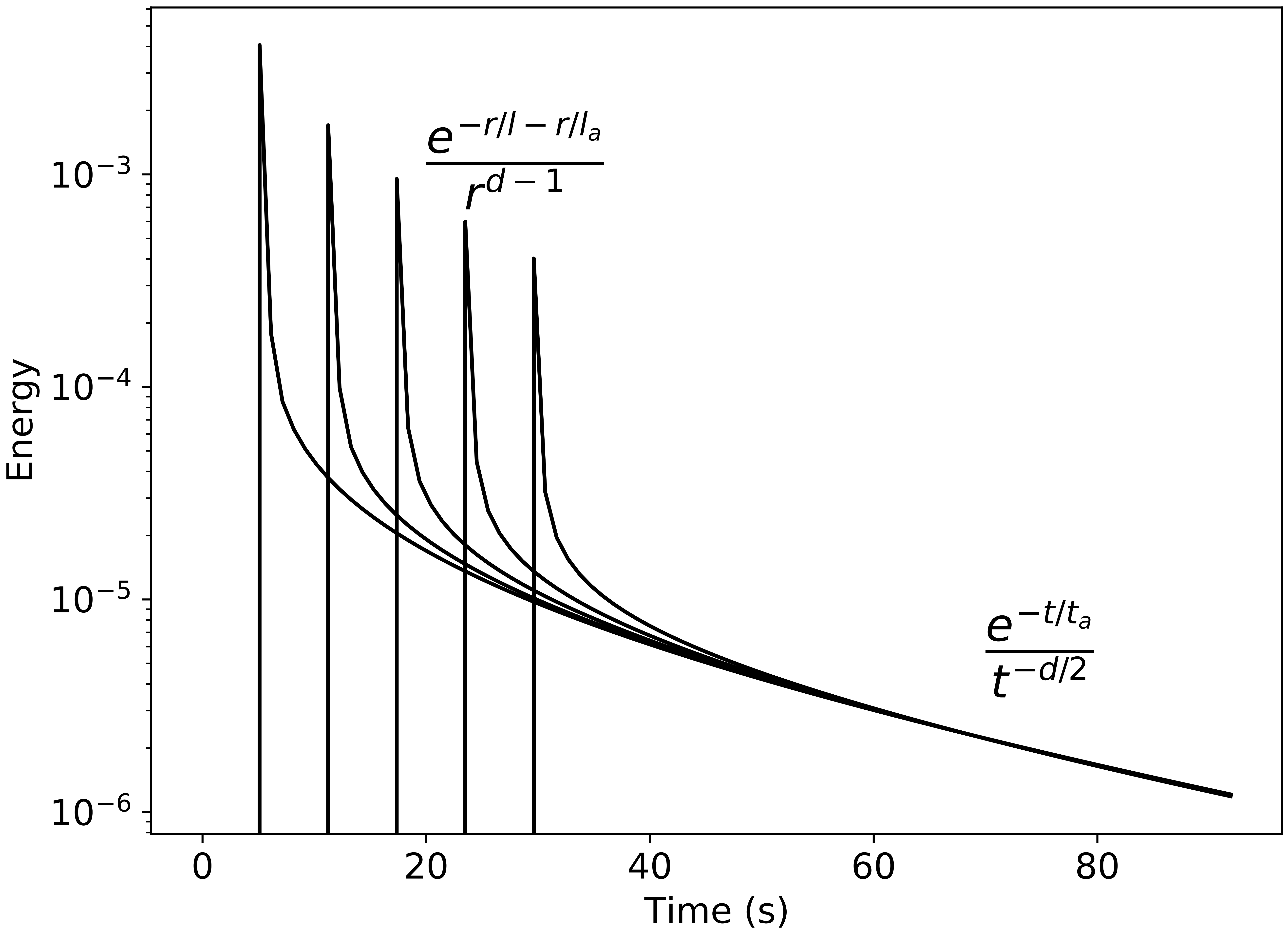

Spatial decay rate of ballistic peak
->Total attenuation
Temporal decay rate of the coda:
->Absorption

« Multiple Lapse-Time Window Analysis » of Sato, Fehler and Hoshiba (1992, 1993)

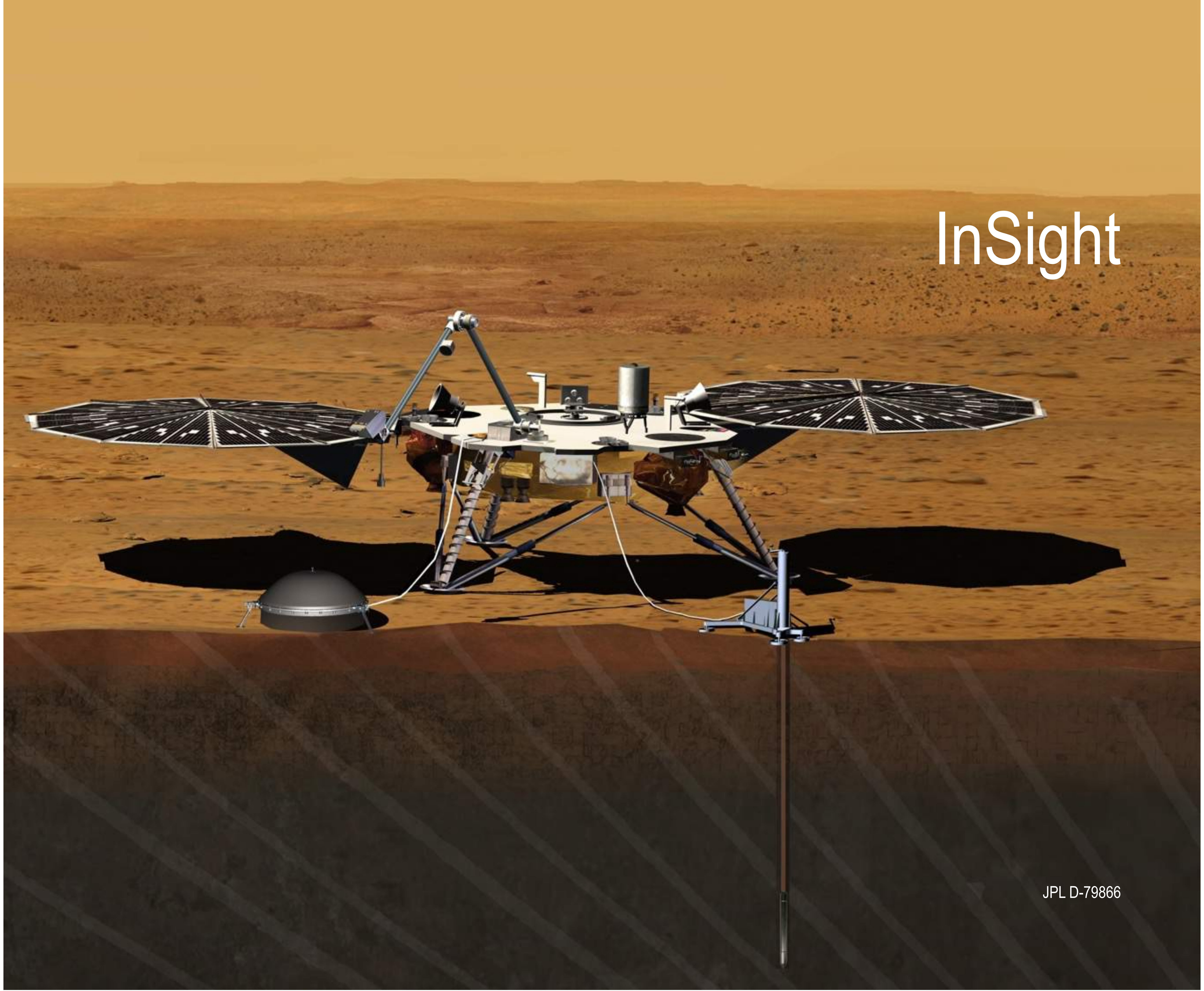
InSight
JPL D-79866

Seismic Events Reported by Mars Quake Service

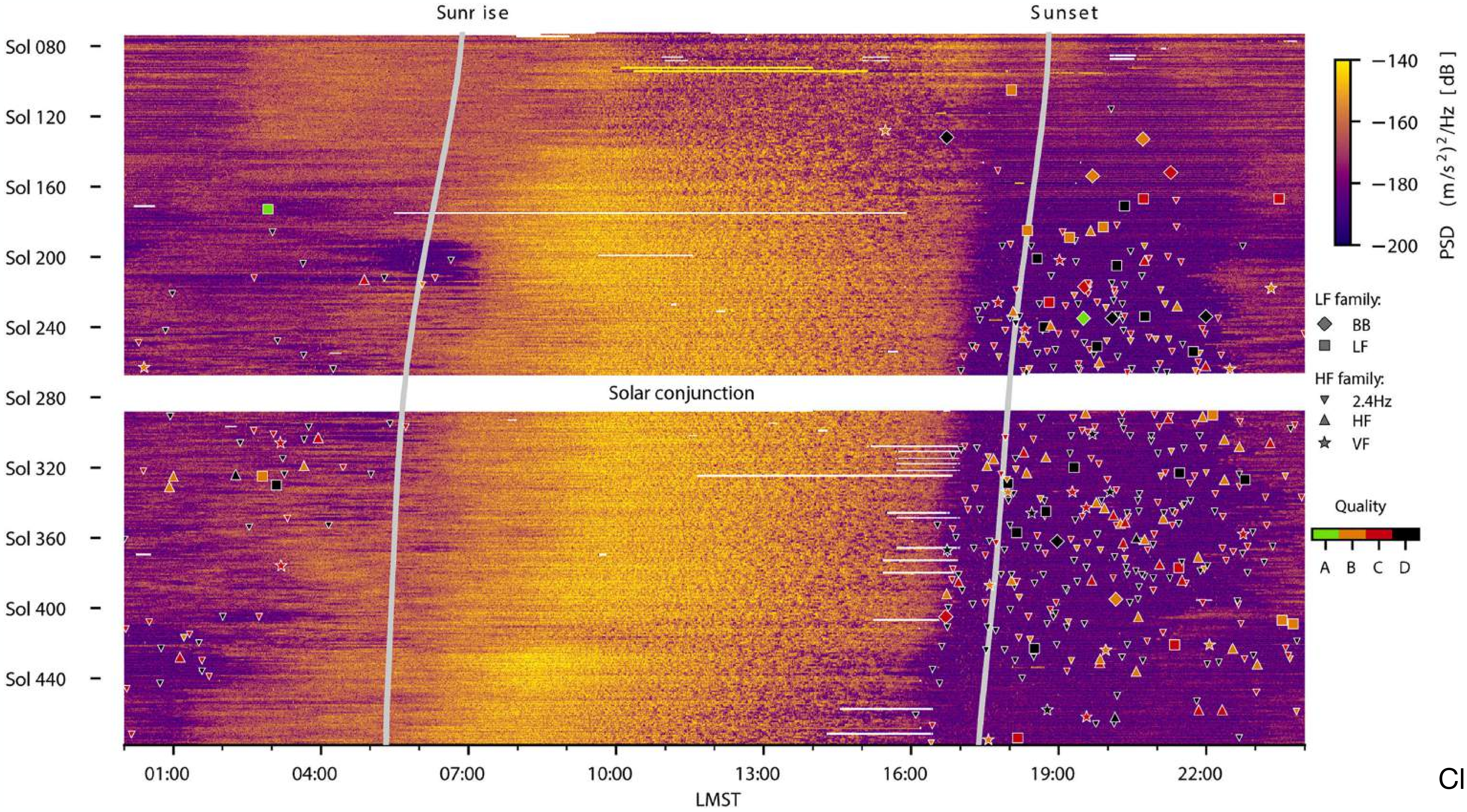

Clinton et al, 2021

Seismic Events Reported by Mars Quake Service

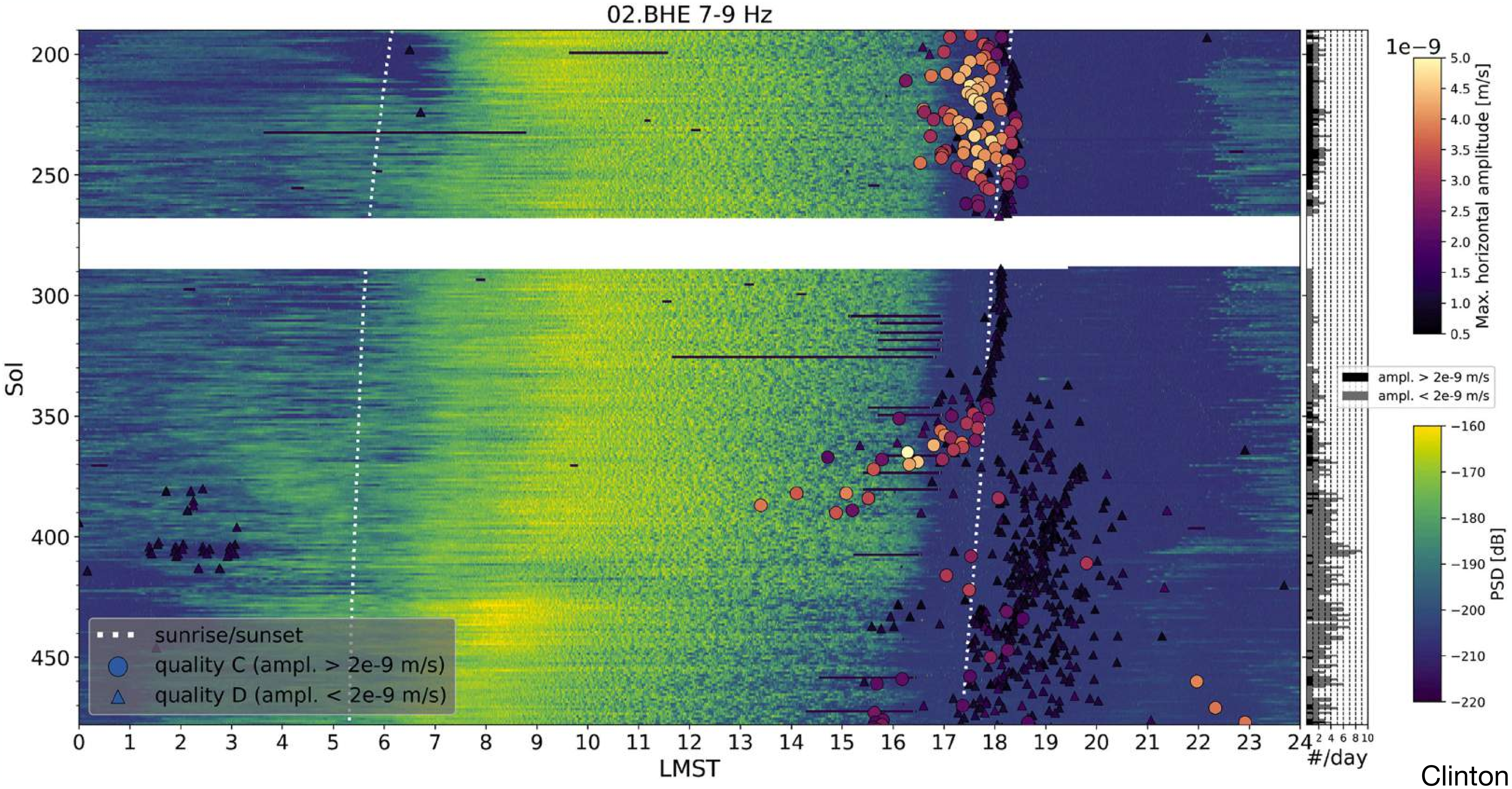

Clinton et al, 2021

VF event (S0334a) observation

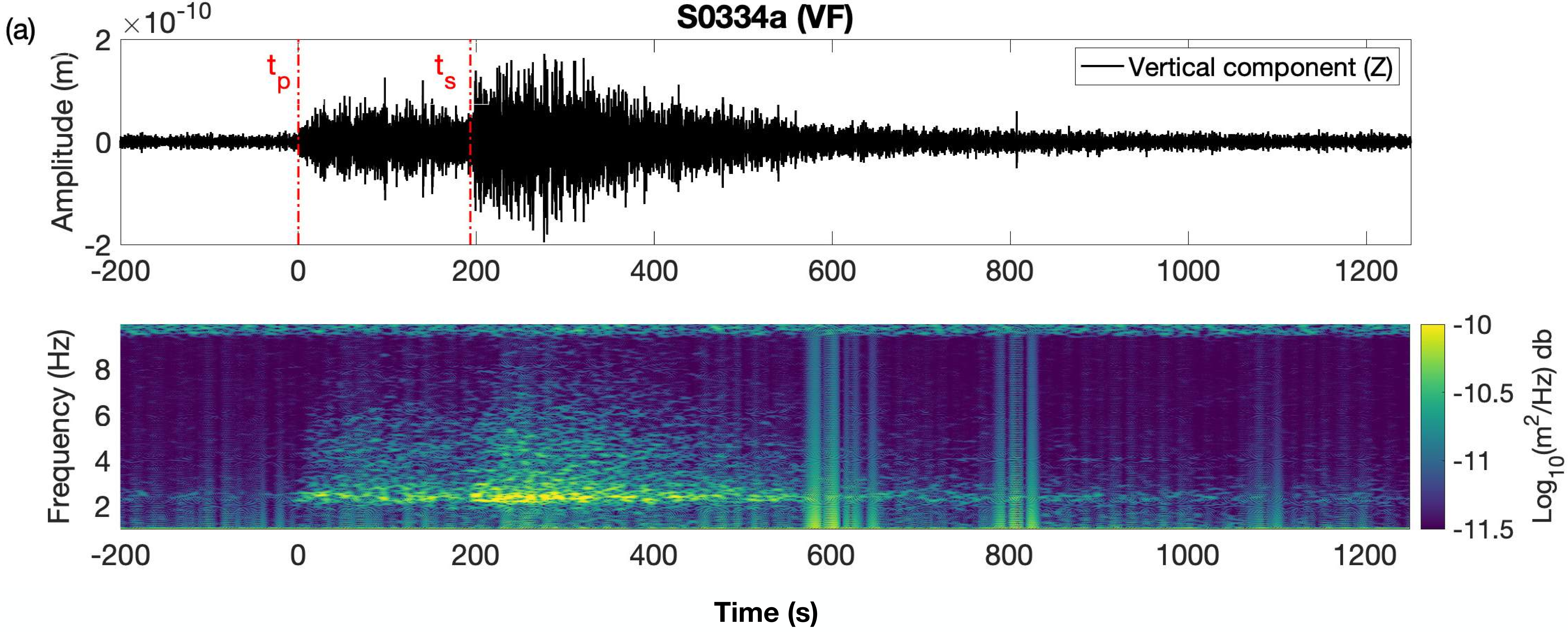

Menina et al., 2021

Separation of Scattering and Absorption

Iterative Linearised Inversion

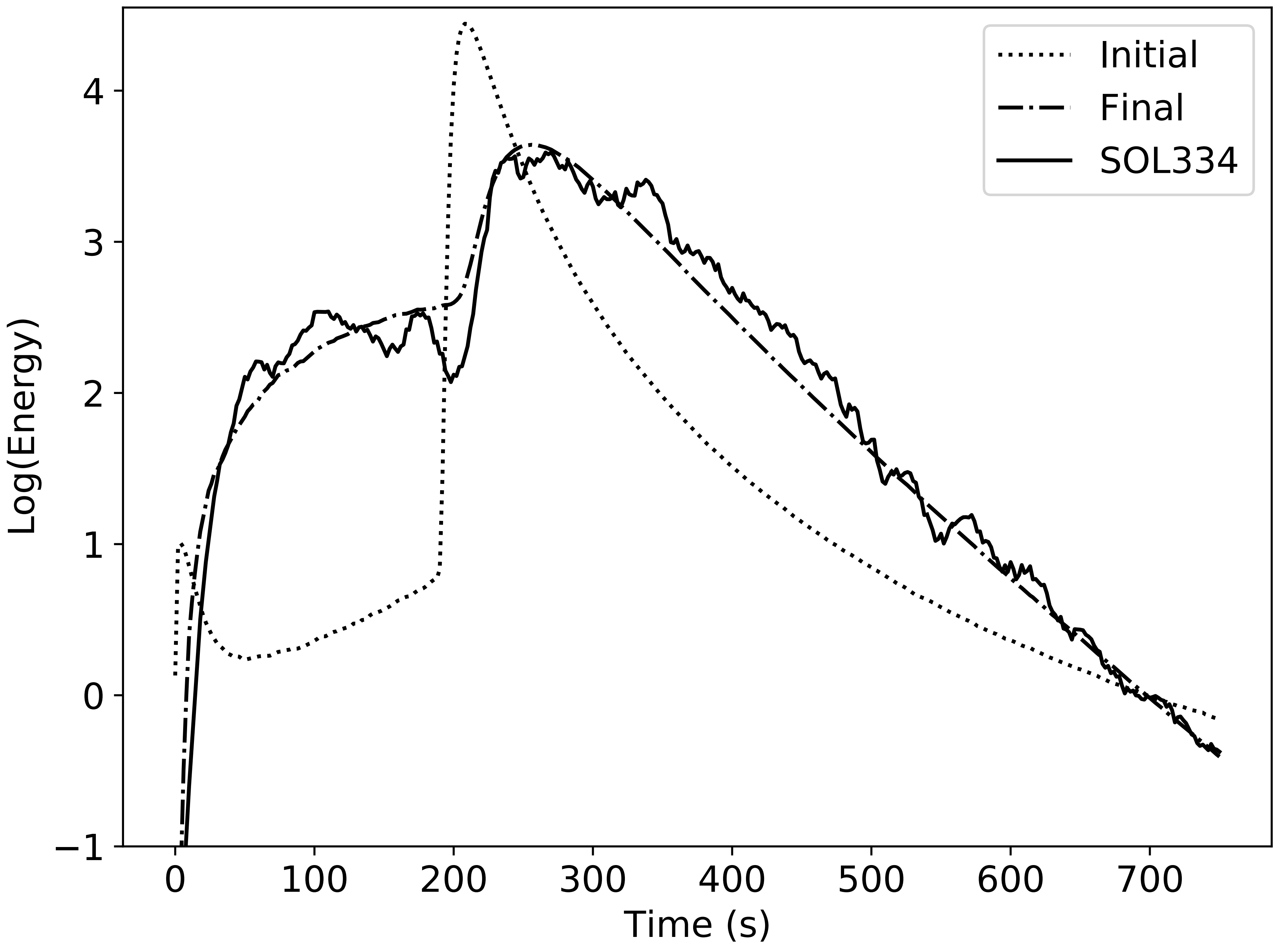

Partial Derivatives of Envelopes

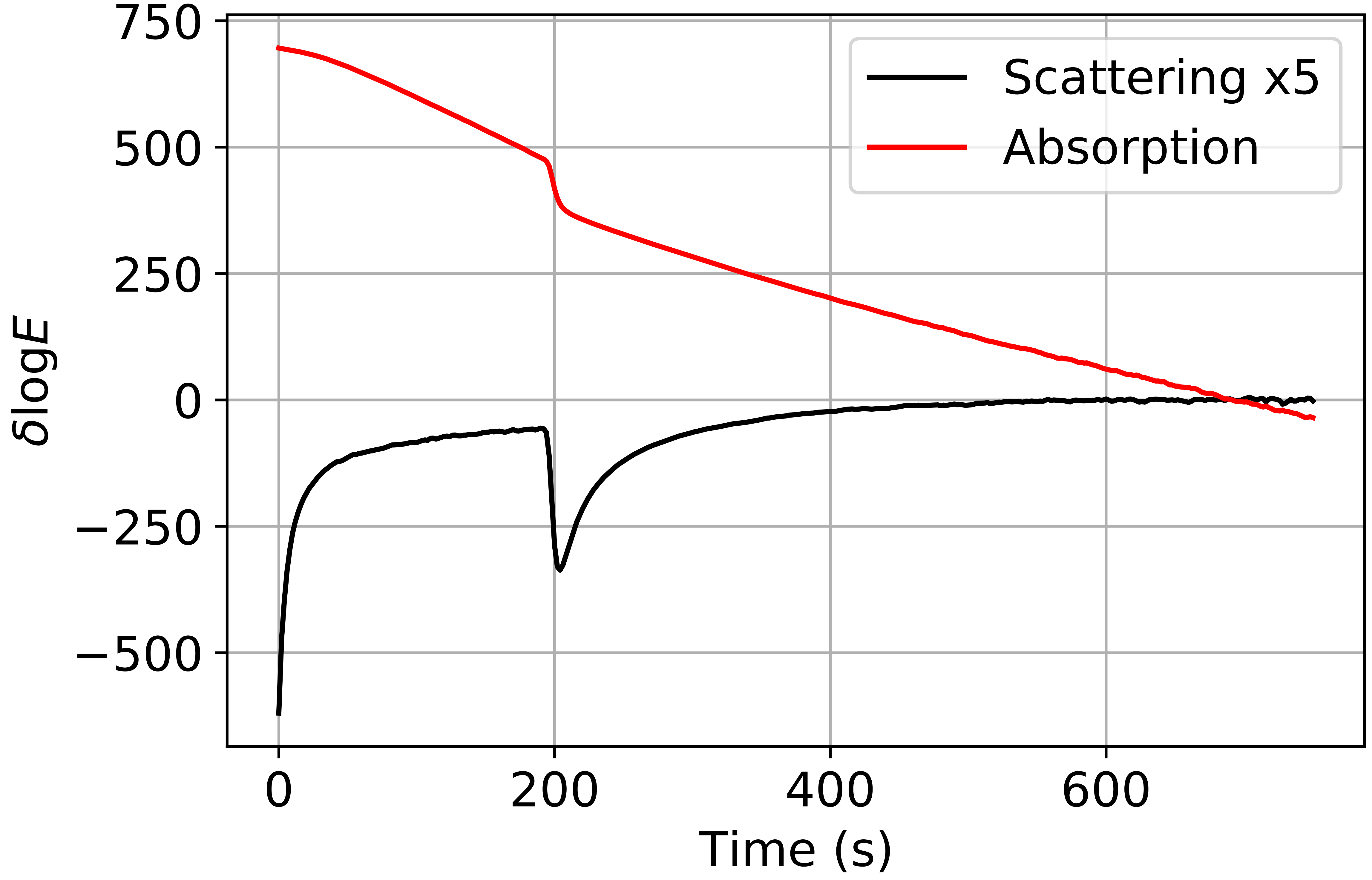

Menina et al., 2021

Inversion of 8 VF Events

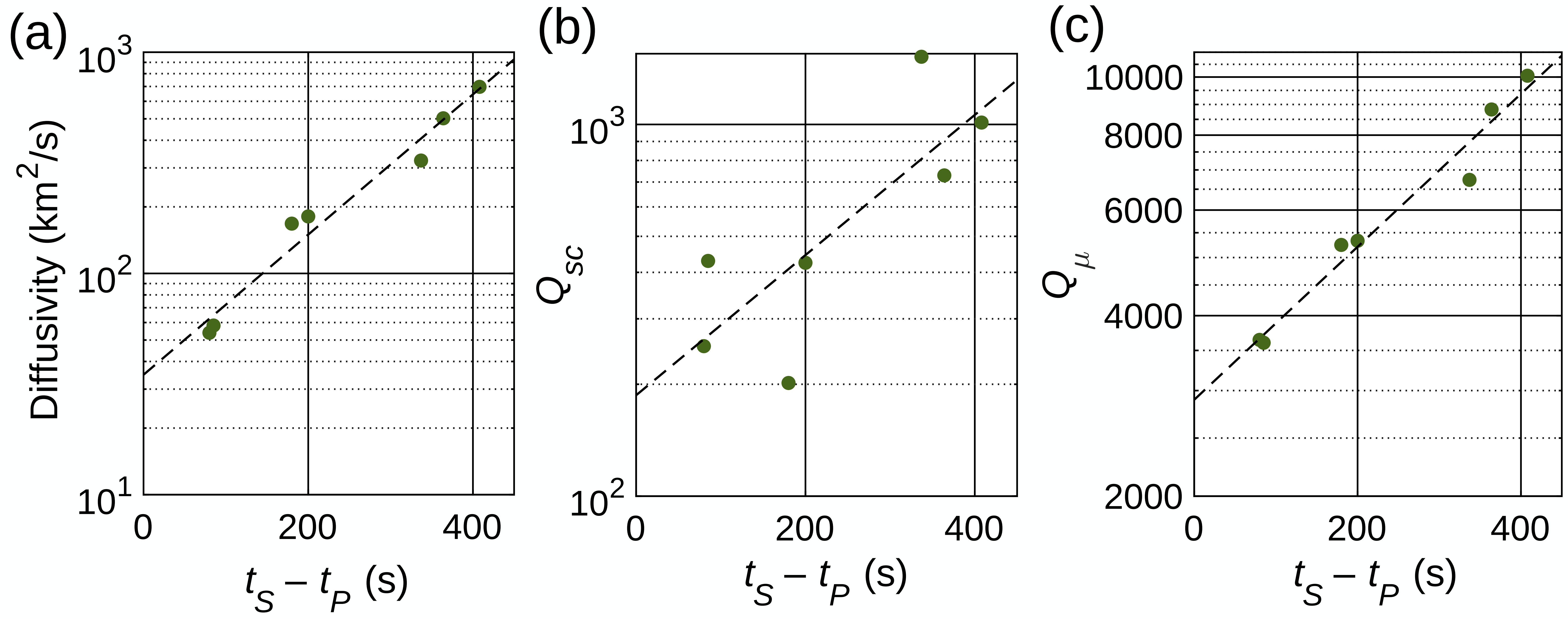

Very High Q suggests propagation in a dry medium

Apparent attenuation decreases with hypocentral distance

-> Stratified Models

Menina et al., 2021

Detection of velocity changes in the lunar regolith

Green's Function Reconstruction from Ambient Vibrations

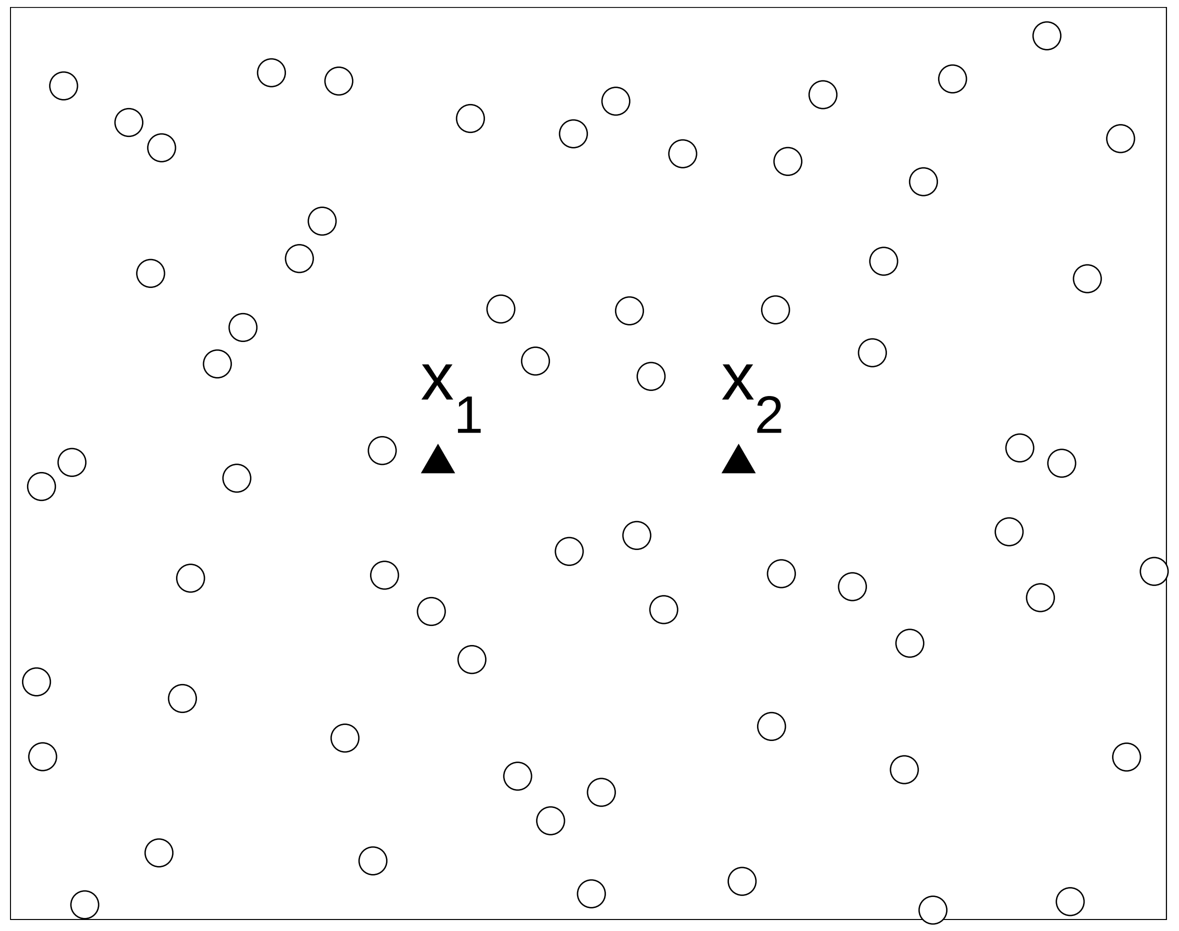

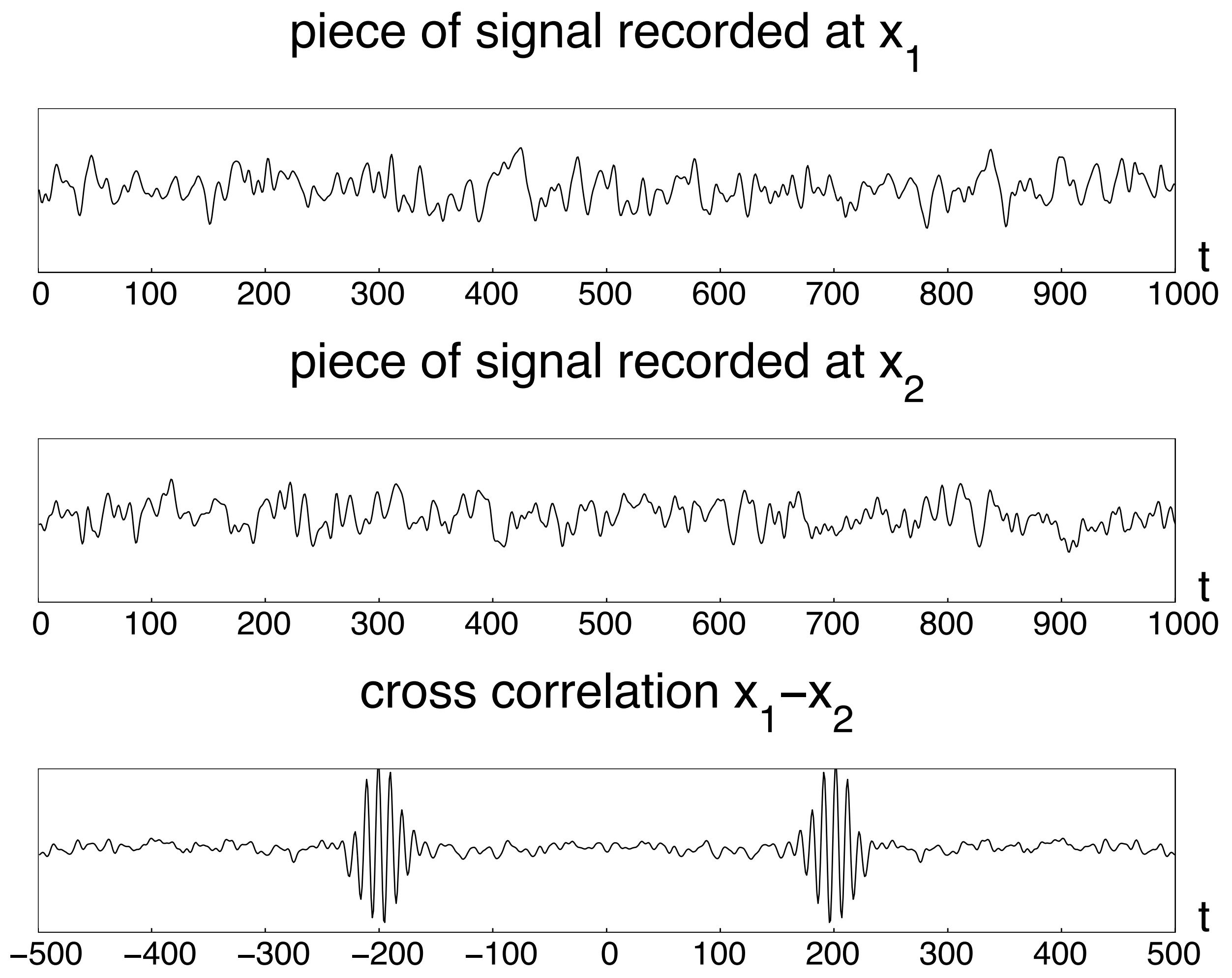

Stehly, PhD thesis

Apollo Data

Ballistic Rayleigh Wave

Coda

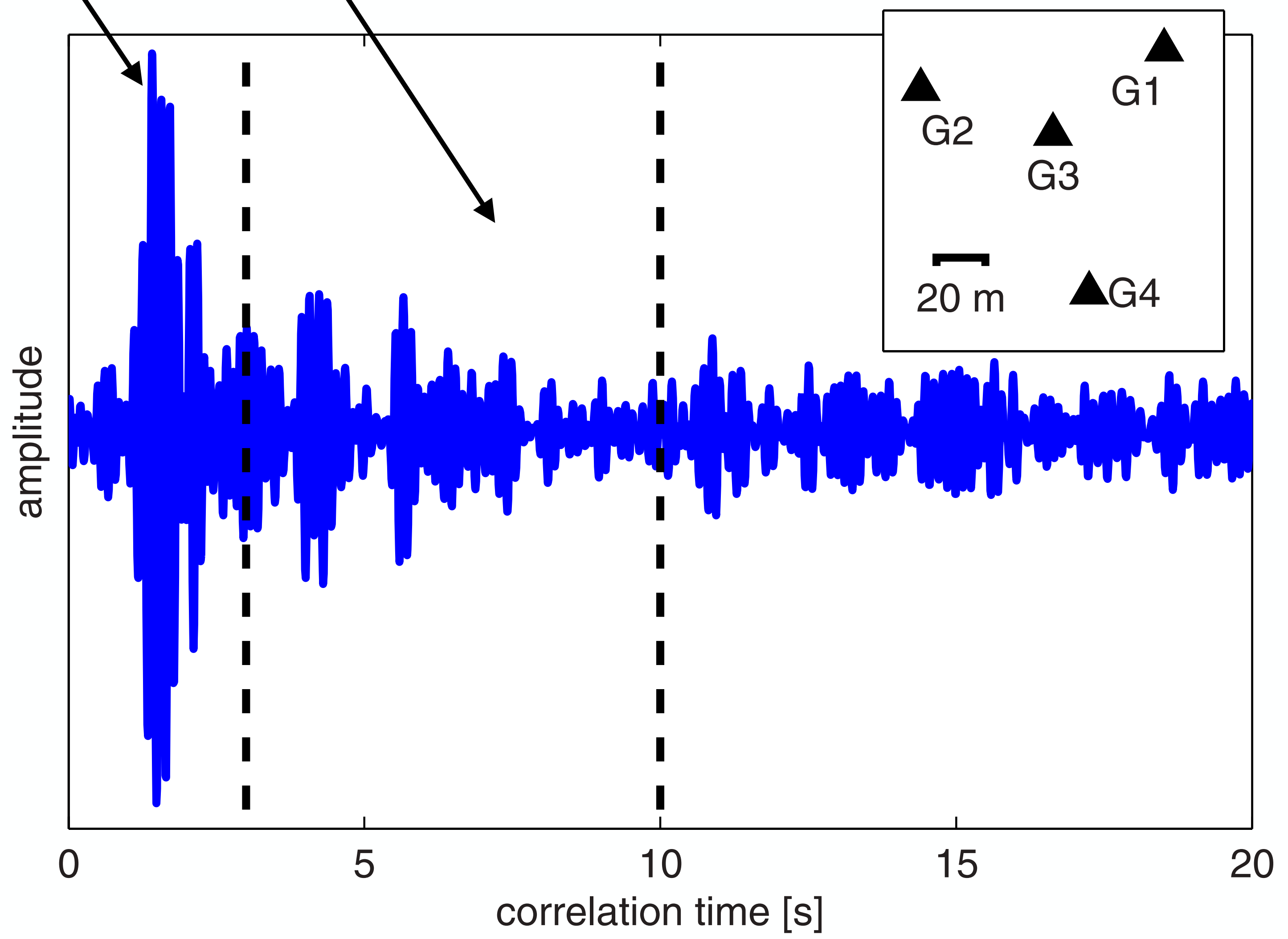

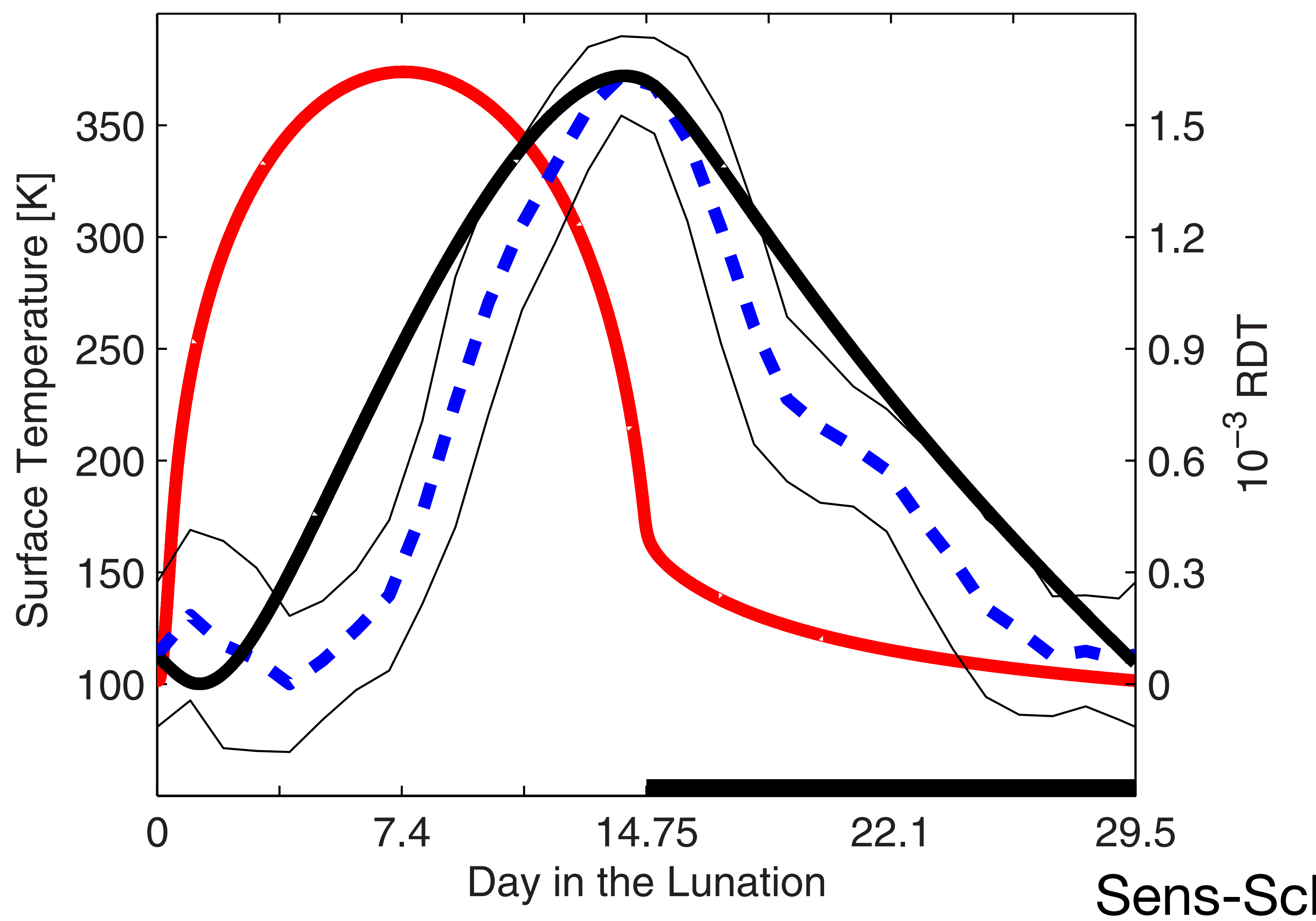

Coda Relative Delay Time

Sens-Schoenfelder & Larose, 2008

Phase Delay Between Surface Temperature and Coda Delay Time

Diffusion of Temperature in the Regolith

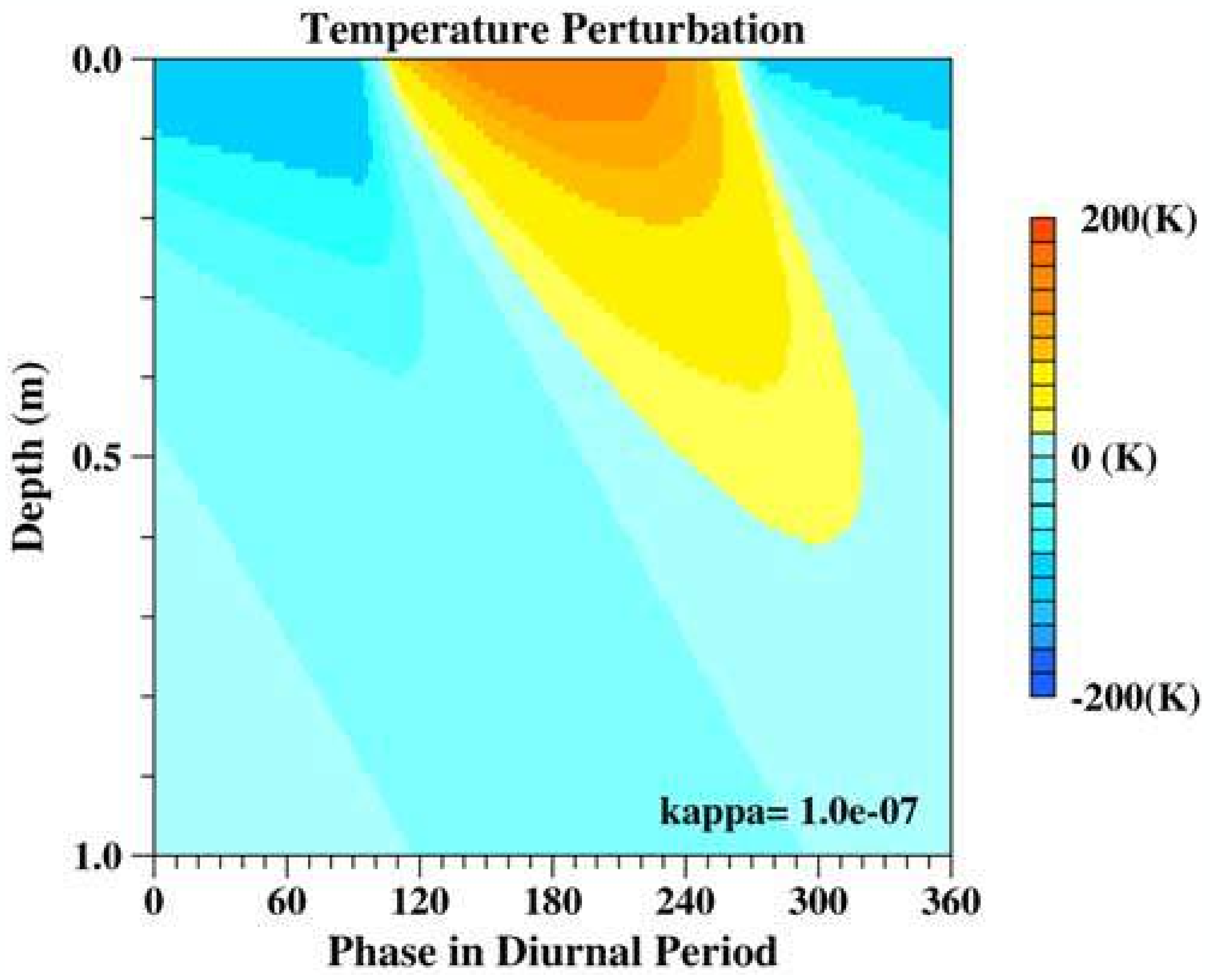

Rayleigh Wave Sensitivity Kernels

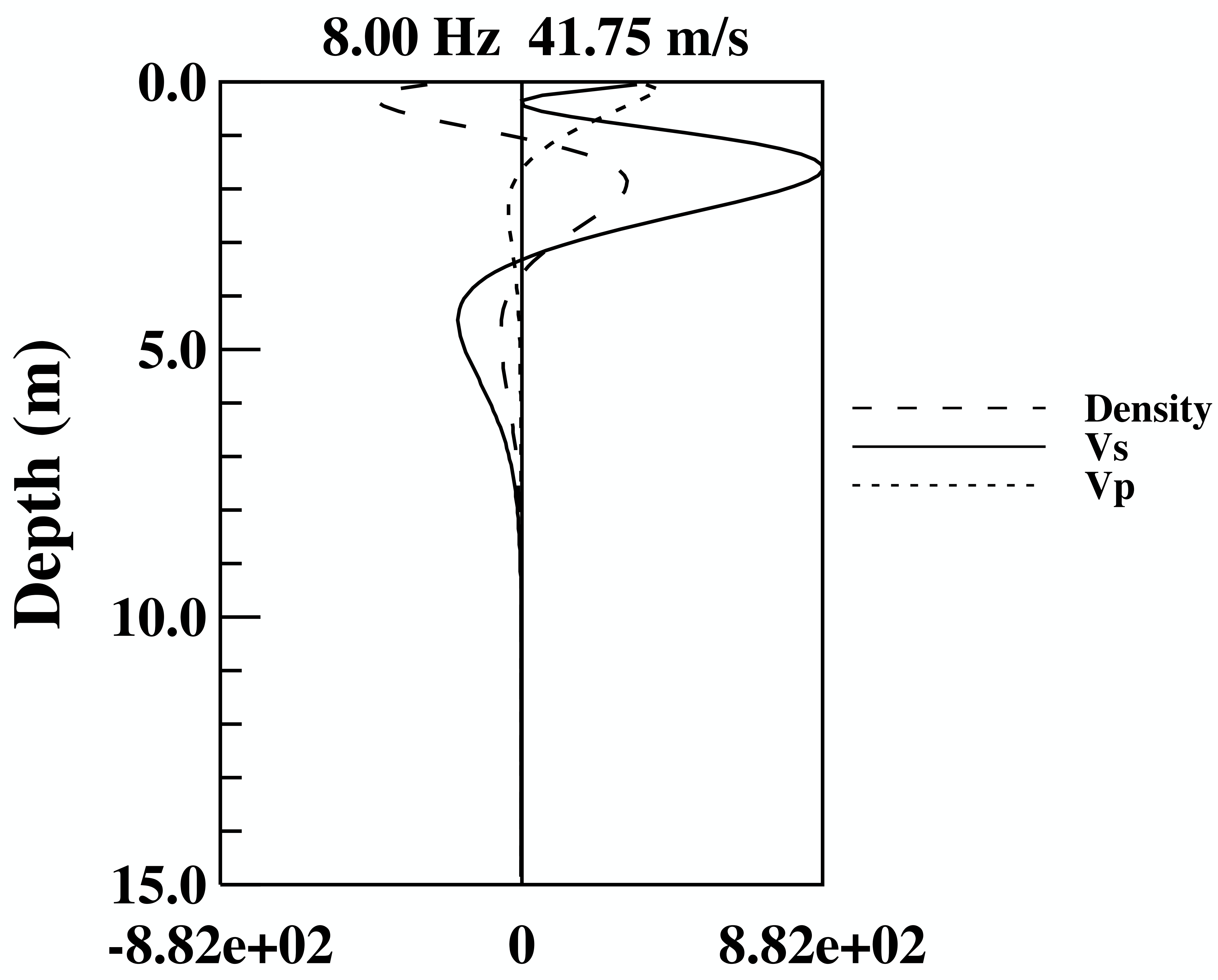

Tanimoto et al., 2008

Evolving Waveforms of SF Events detected by InSight VBB

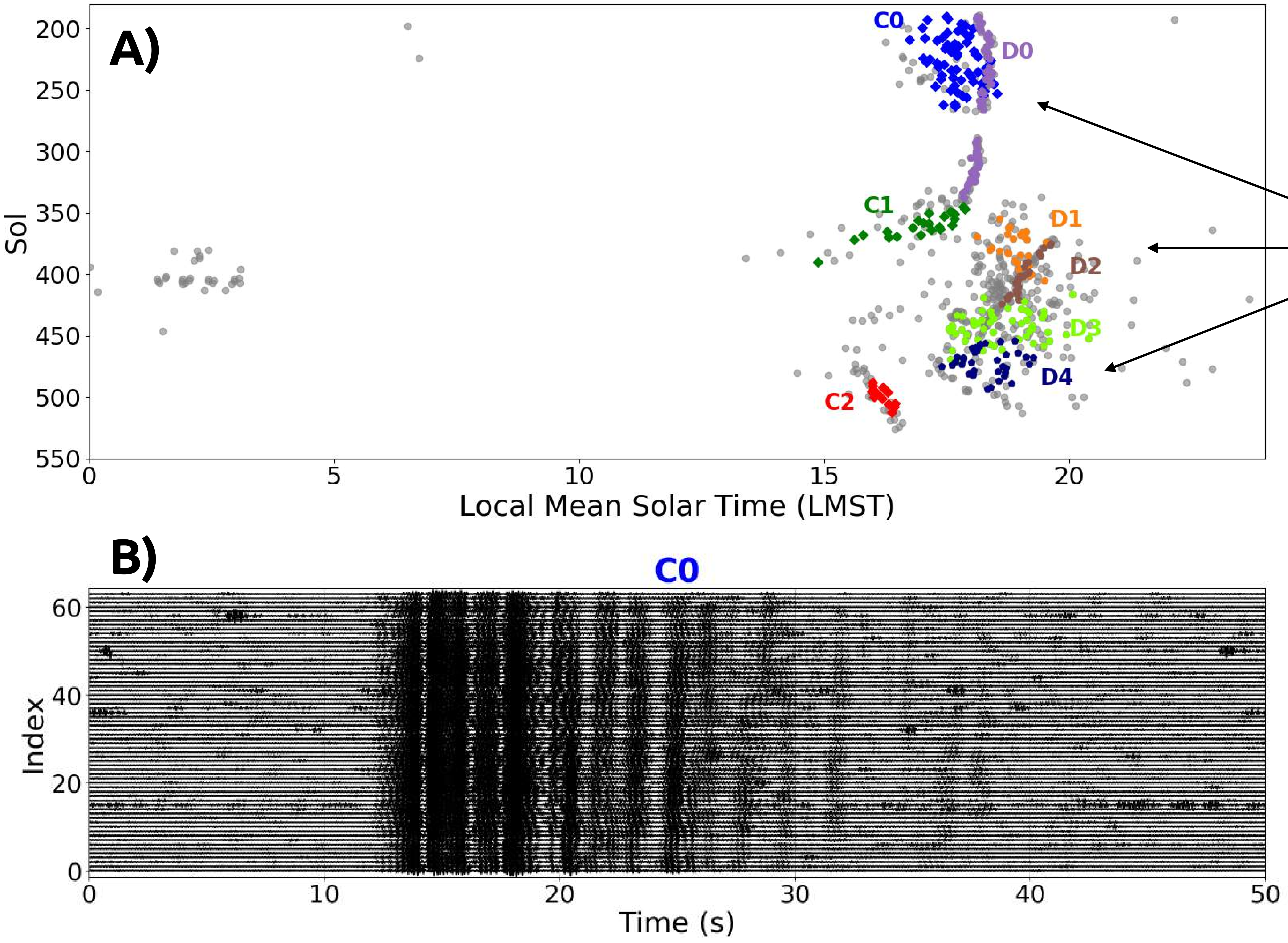

Different clusters of repeating events

Stretching of the waveforms is apparent

Compaire et al., 2022

Waveform changes seen in the frequency domain

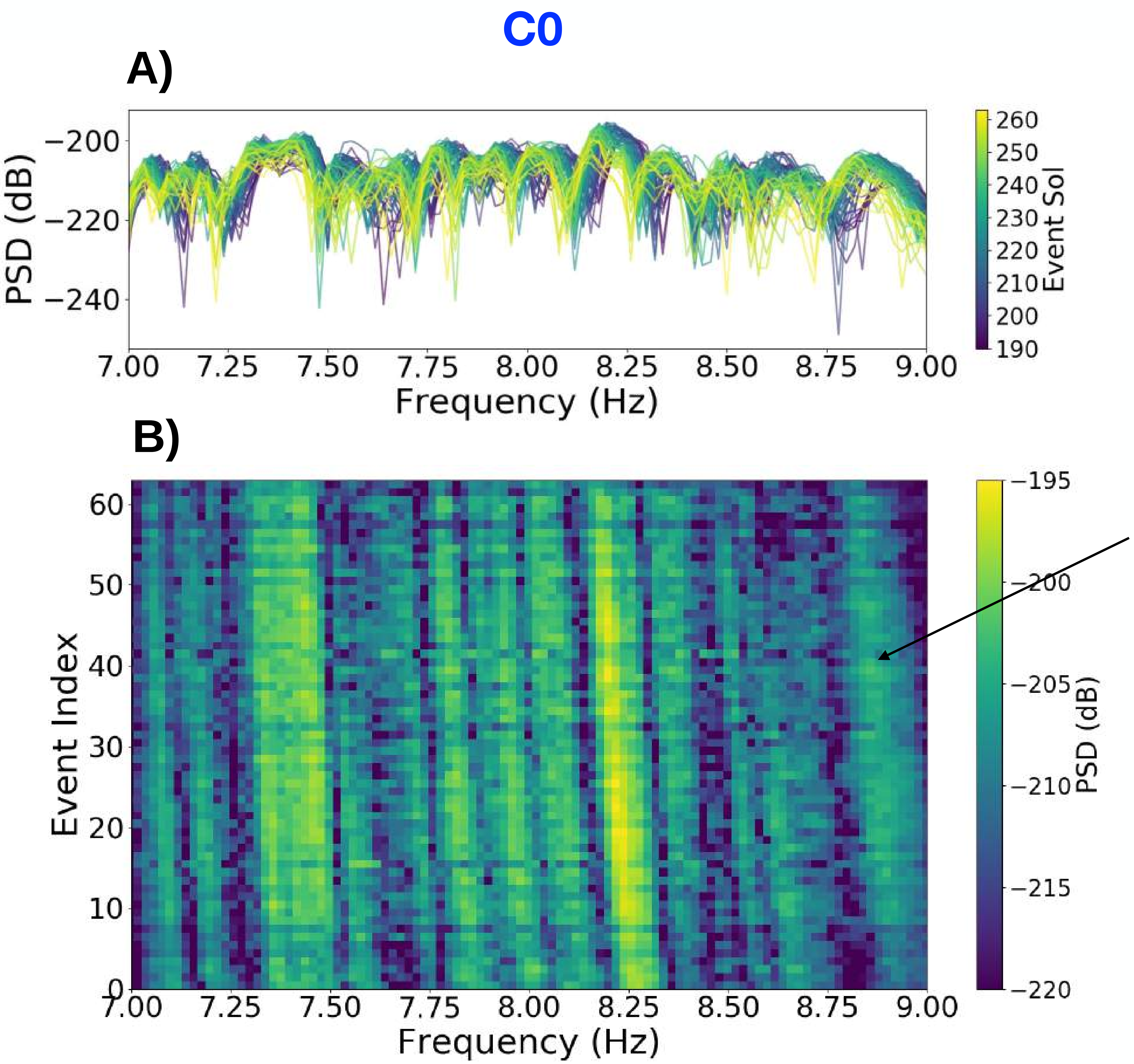

- Stretching in time domain gives compression in frequency domain
- ‘Frequency Band Structure’

Seasonal Variations of Seismic Velocities seen by SF Events

A)

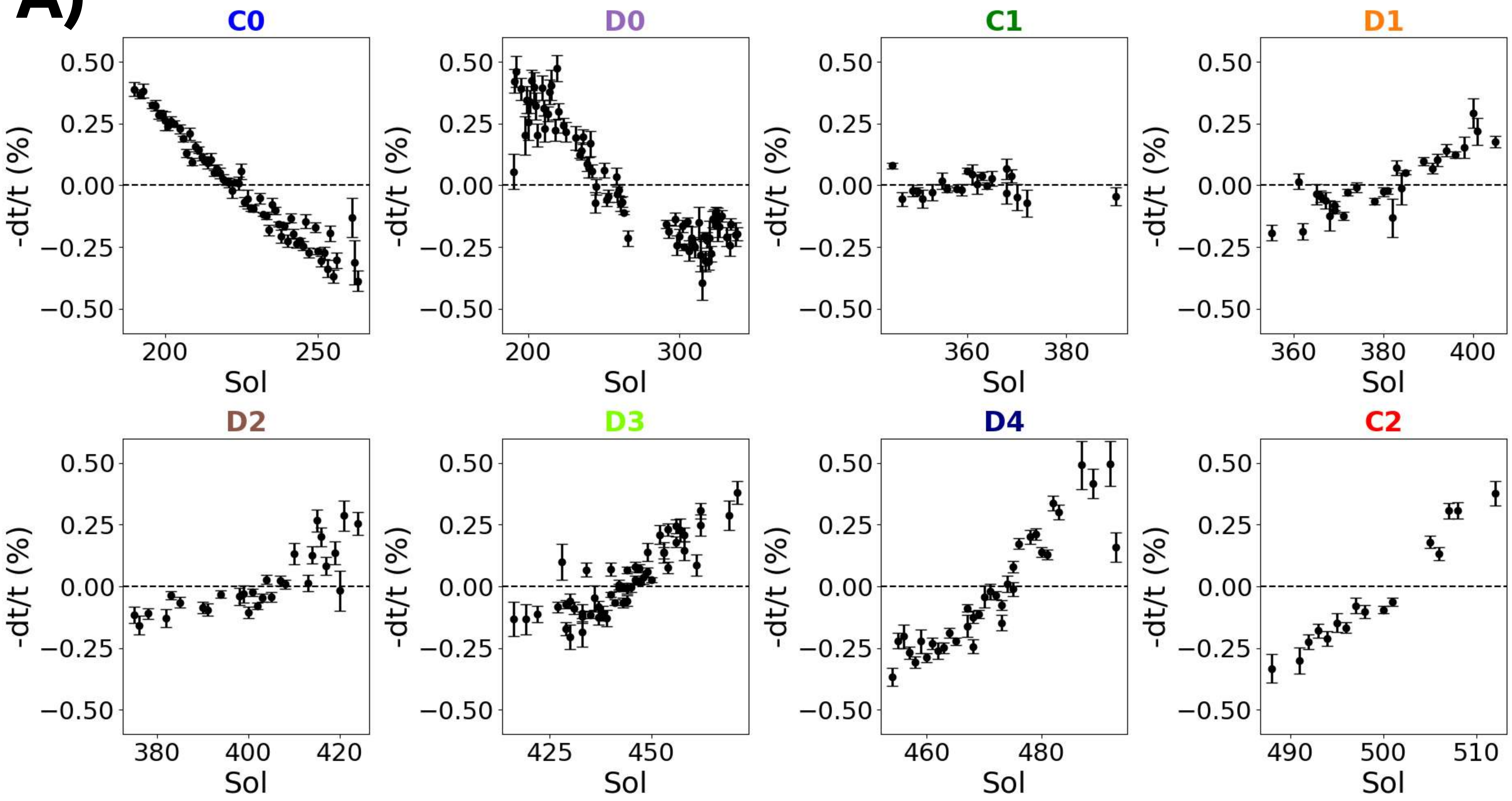

Velocity variations from ambient noise

Lander Resonances

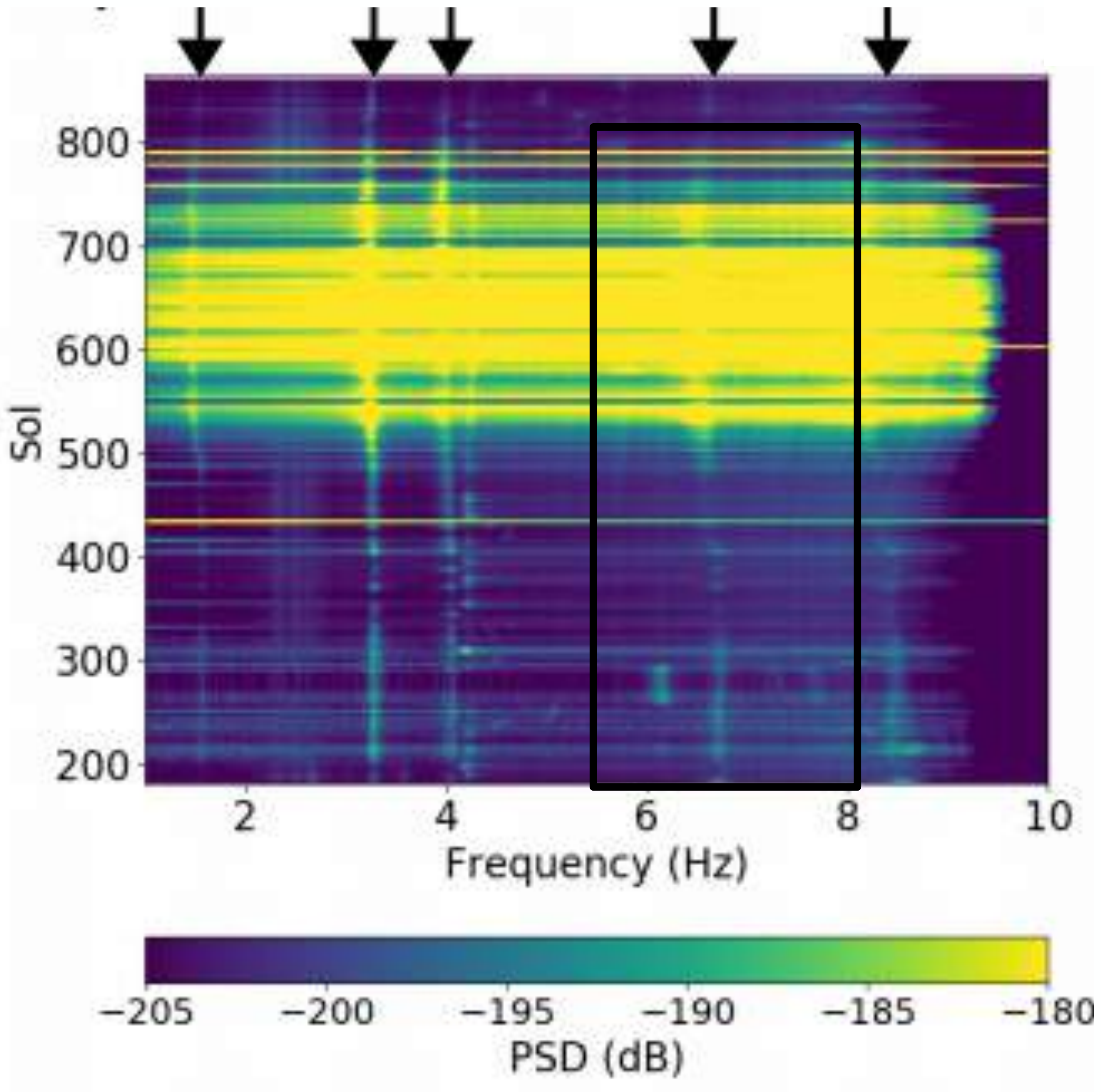

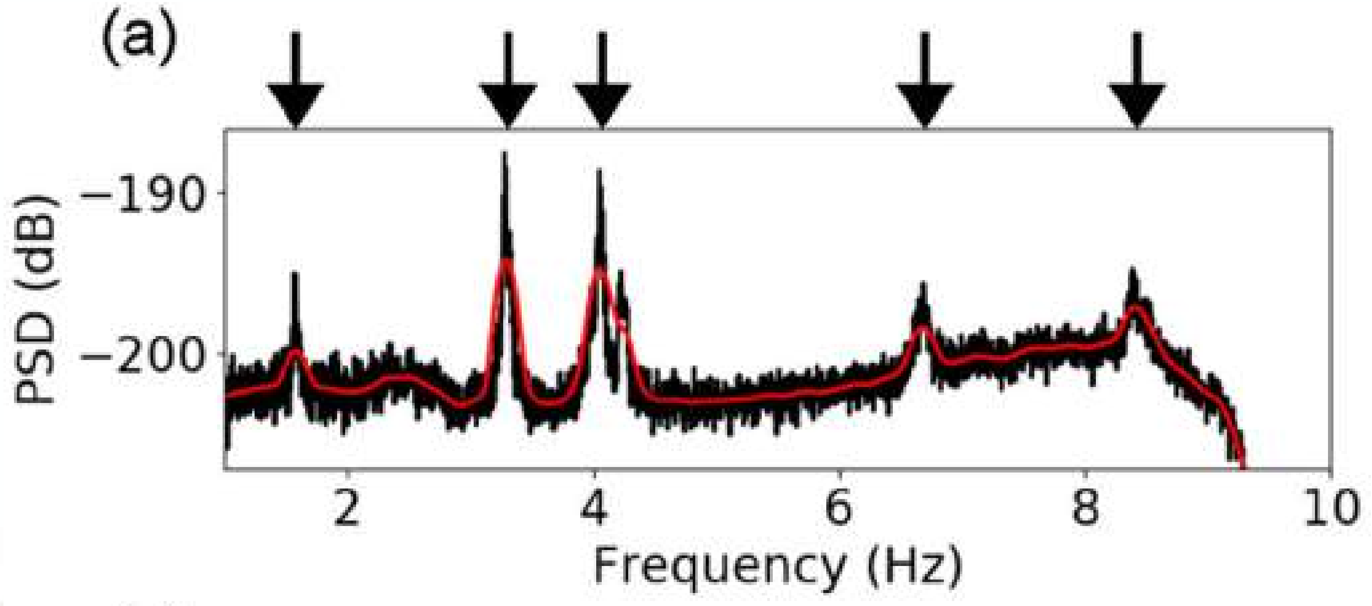

VBB North Component Denoising

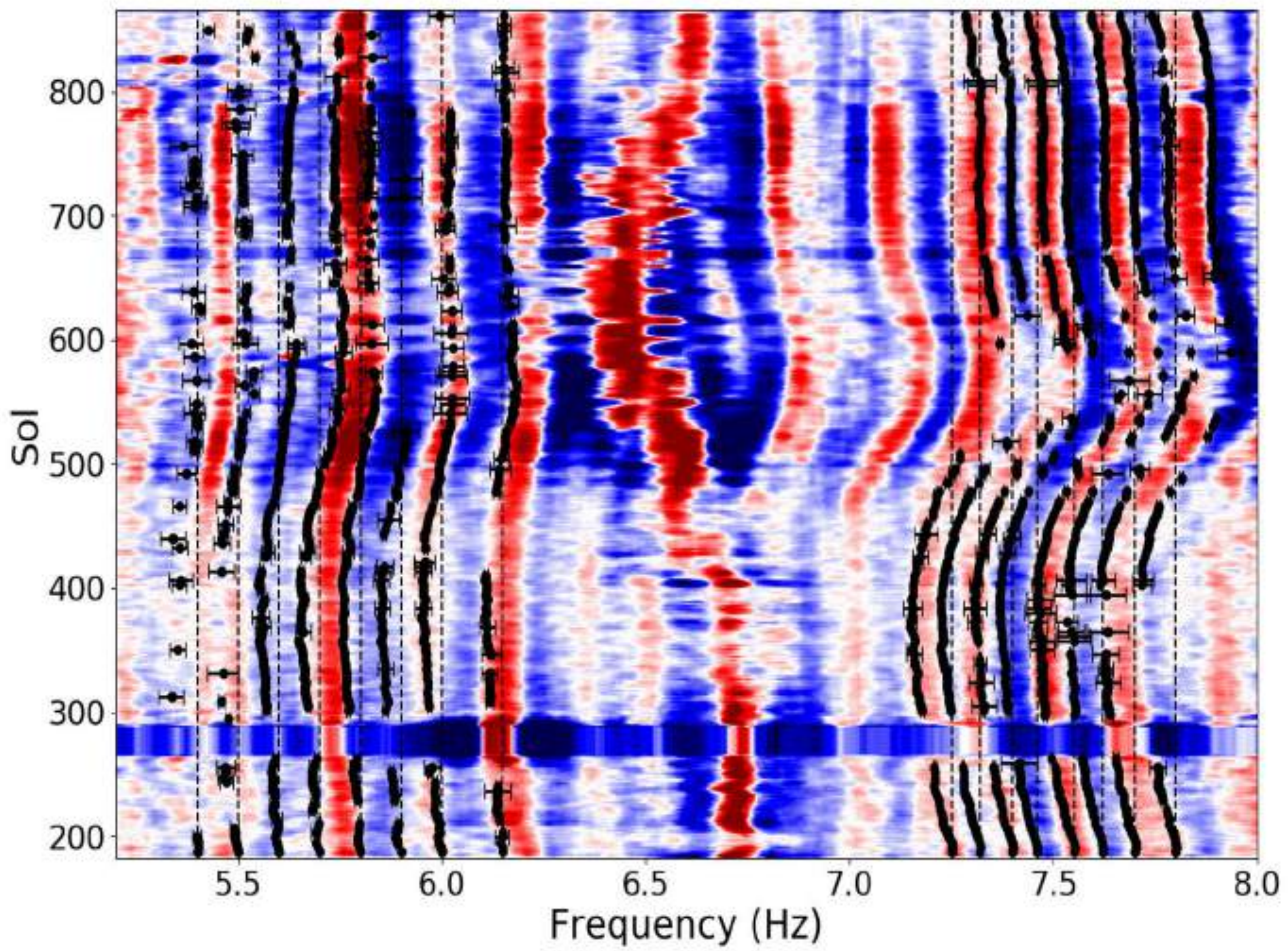

Lander modes prohibit the use of the time-domain cross-correlation method

We track the ‘band structure’ in the frequency domain

Consistent pattern between SF events and ambient noise

The velocity change increases with frequency

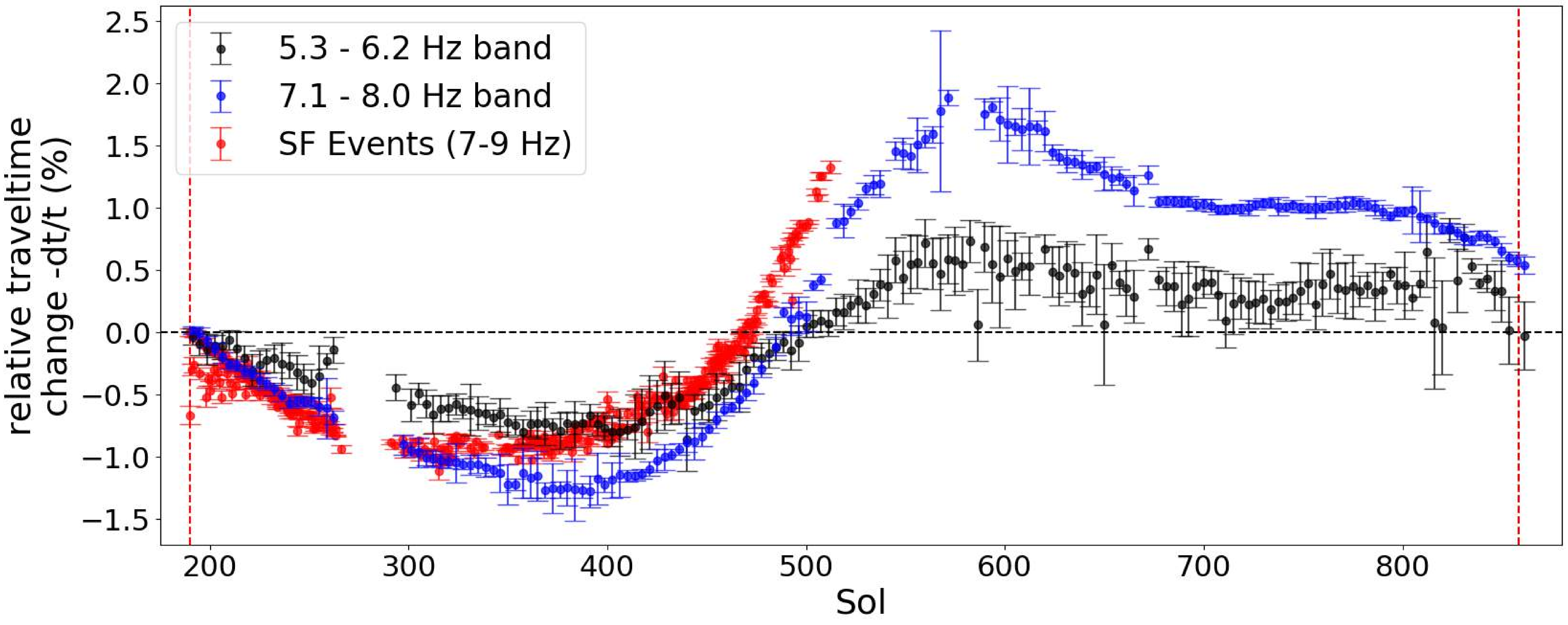

Relation between seasonal temperature variations and velocity

!!! Positive !!! correlation between temperature and velocity

Delay is typically 100 days

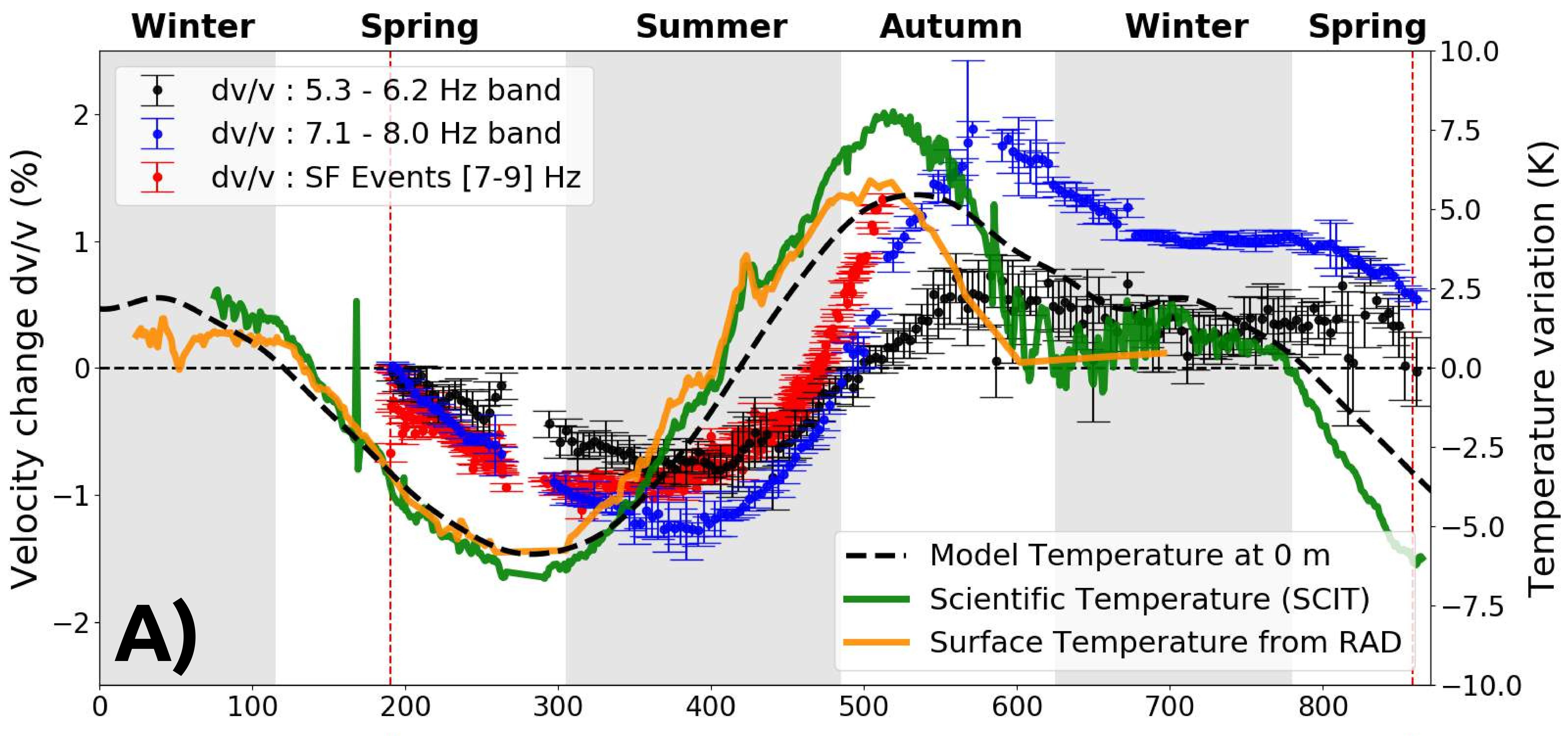

Thermoelastic modeling

VOL. 80, NO. 2 JOURNAL OF GEOPHYSICAL RESEARCH JANUARY 10, 1975

A Note on Thermoelastic Strains and Tilts

JON BERGER

Institute of Geophysics and Planetary Physics, University of California, San Diego
La Jolla, California 92037

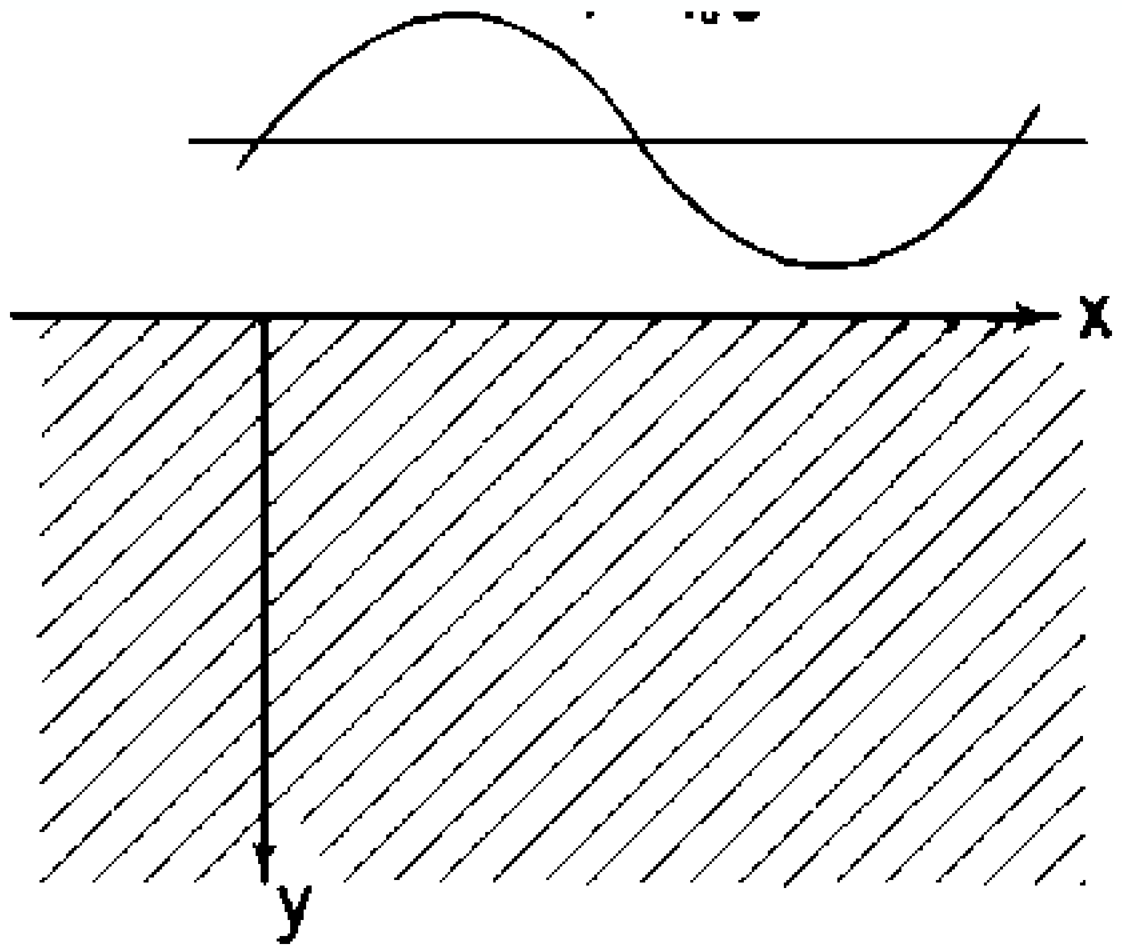

$$\frac{\Delta v}{v}(x, z, t) = -2\alpha b \frac{\partial \rho v^2}{\partial \sigma} \sum_{\omega} T_\omega \cos(k_x x) \Bigg[\cos(\omega t + \phi_\omega - \gamma z) e^{-\gamma z} - \frac{(1+\nu)}{\sqrt{2\gamma^2 + 2\gamma k_x + k_x^2}} \cos(\omega t + \phi_\omega - \psi) k_x e^{-k_x z} \Bigg],$$

$$\tan \psi = \frac{\gamma}{\gamma + k_x} \quad \text{with } \psi \in [0, \pi/2[$$

To make the link with seismic observations we assume the signal of SF events is dominated by Rayleigh waves with Cs=100m/s and nu=0.2

Comparison between thermo-elastic model and data

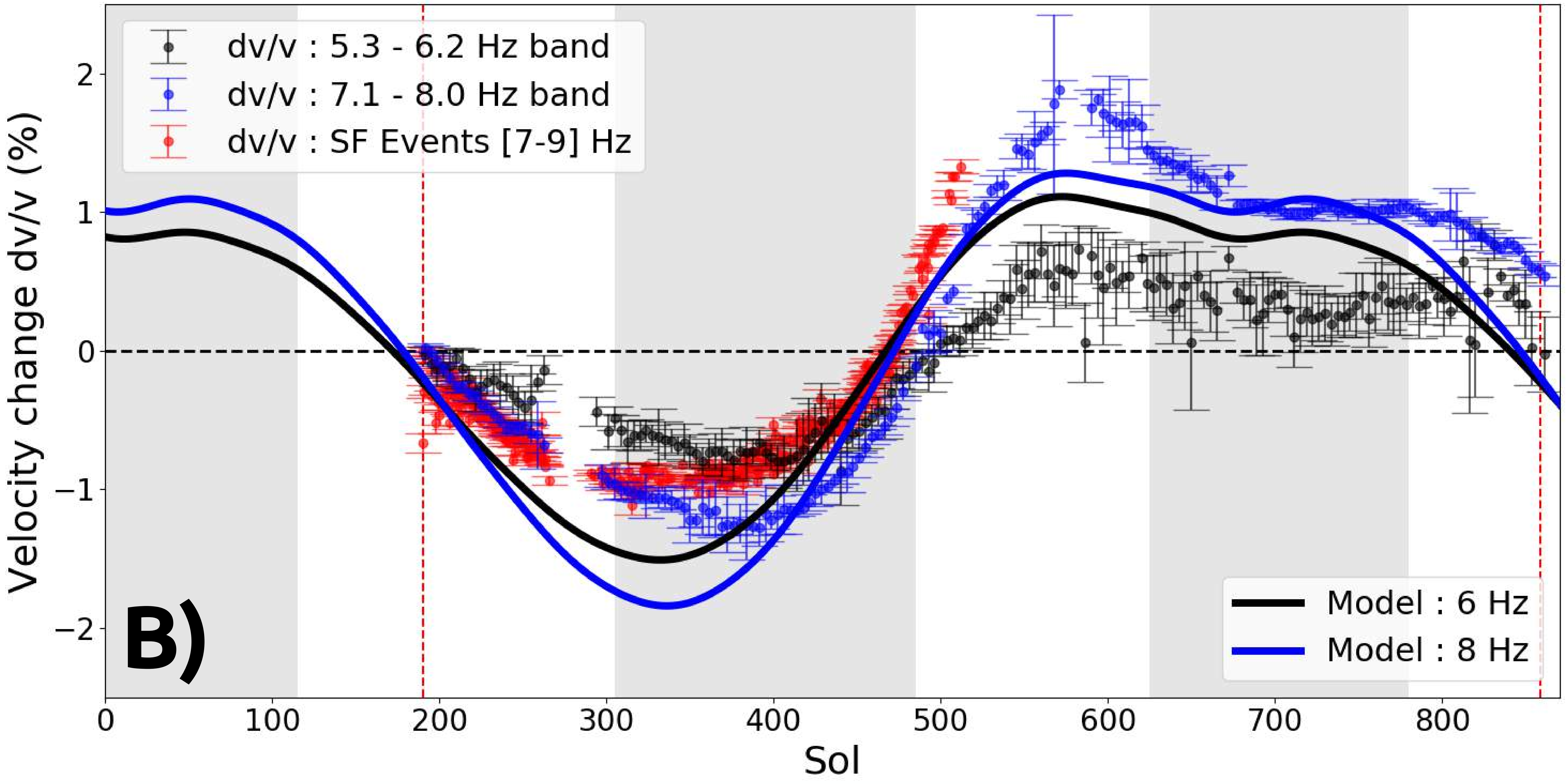

Compaire et al., 2022

- Delay with surface temperature is a bit too small
- General asymmetry is well reproduced
- Sharp contrast with lunar observations
- Frequency dependence not OK

->Body wave/ surface wave partition?

Phenomenological Transport Model for coupled surface/body waves in a half-space

$$(\partial_t + v_g \widehat{\mathbf{n}} \cdot \nabla)\, e_s(t, \mathbf{r}, z, \widehat{\mathbf{n}}) = -\frac{e_s(t, \mathbf{r}, z, \widehat{\mathbf{n}})}{\tau^s} + \frac{1}{\tau^{s \to s}} \int_{2\pi} p^{s \to s}(\widehat{\mathbf{n}}, \widehat{\mathbf{n}}')\, e_s(t, \mathbf{r}, z, \widehat{\mathbf{n}}')\, d\hat{n}'$$
$$+ \boxed{\frac{1}{\tau^{b \to s}(z)} \int_{4\pi} p^{b \to s}(\widehat{\mathbf{n}}, \widehat{\mathbf{k}}')\, e_b(t, \mathbf{r}, z, \widehat{\mathbf{k}}')\, d\hat{k}'} + s_s(t, \mathbf{r}, z, \widehat{\mathbf{n}})$$

$$\left(\partial_t + c \widehat{\mathbf{k}} \cdot \nabla\right) e_b(t, \mathbf{r}, z, \widehat{\mathbf{k}}) = -\frac{e_b(t, \mathbf{r}, z, \widehat{\mathbf{k}})}{\tau^b(z)} + \frac{1}{\tau^{b \to b}} \int_{4\pi} p^{b \to b}(\widehat{\mathbf{k}}, \widehat{\mathbf{k}}')\, e_b(t, \mathbf{r}, z, \widehat{\mathbf{k}}')\, d\hat{k}'$$
$$+ \boxed{\frac{1}{\tau^{s \to b}} \int_{2\pi} p^{s \to b}(\widehat{\mathbf{k}}, \widehat{\mathbf{n}}')\, e_s(t, \mathbf{r}, z, \widehat{\mathbf{n}}')\, d\hat{n}'} + s_b(t, \mathbf{r}, z, \widehat{\mathbf{n}})$$

$$\text{B.C.}: \; e_b(t, \mathbf{r}, 0, \widehat{\mathbf{k}}_i) = e_b(t, \mathbf{r}, 0, \widehat{\mathbf{k}}_r)$$

Margerin, Barajas & Campillo, 2019

Equipartition between Surface and Body Waves

Uniformly scattering half-space

- Monte-Carlo Simulations

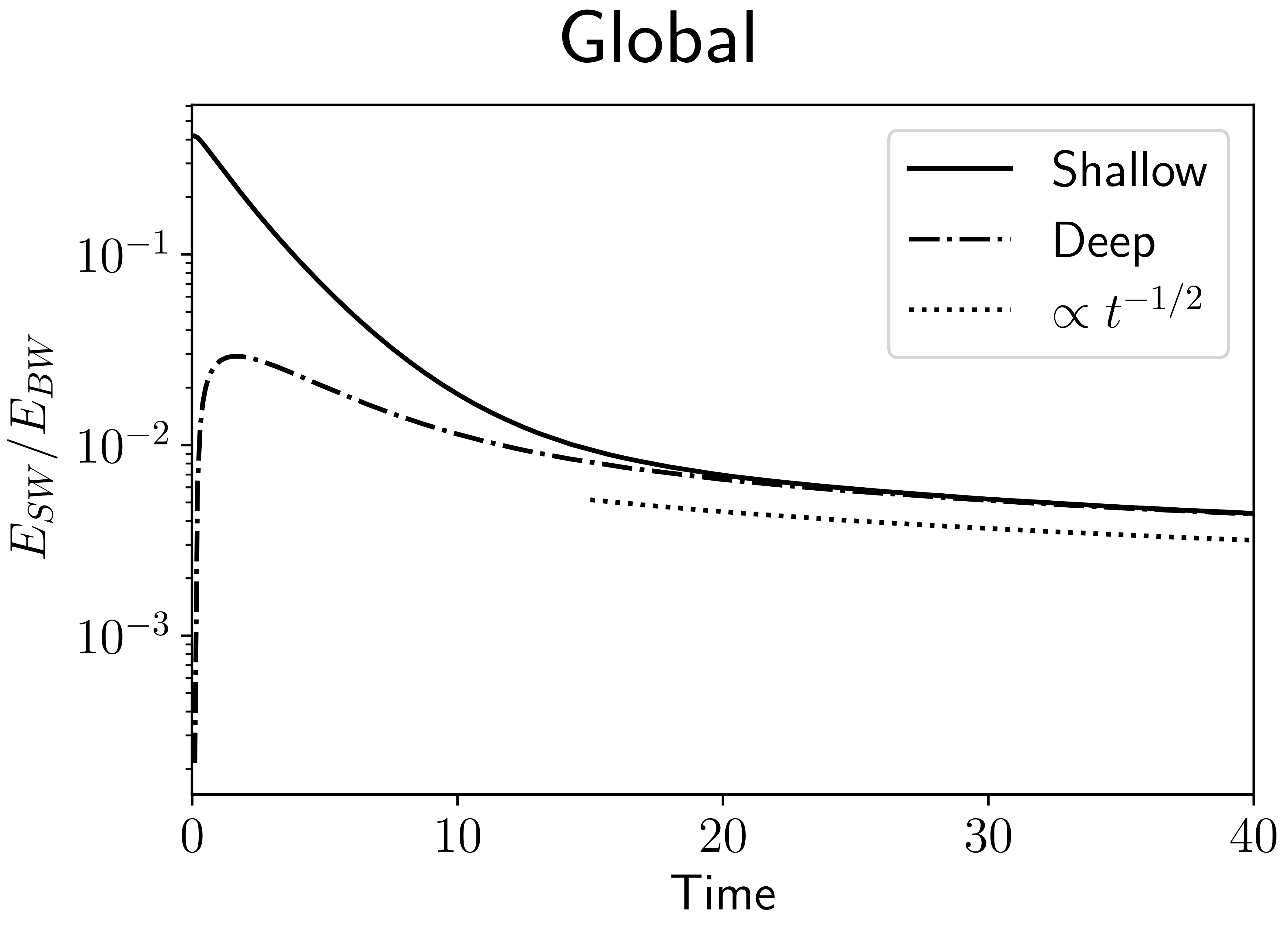

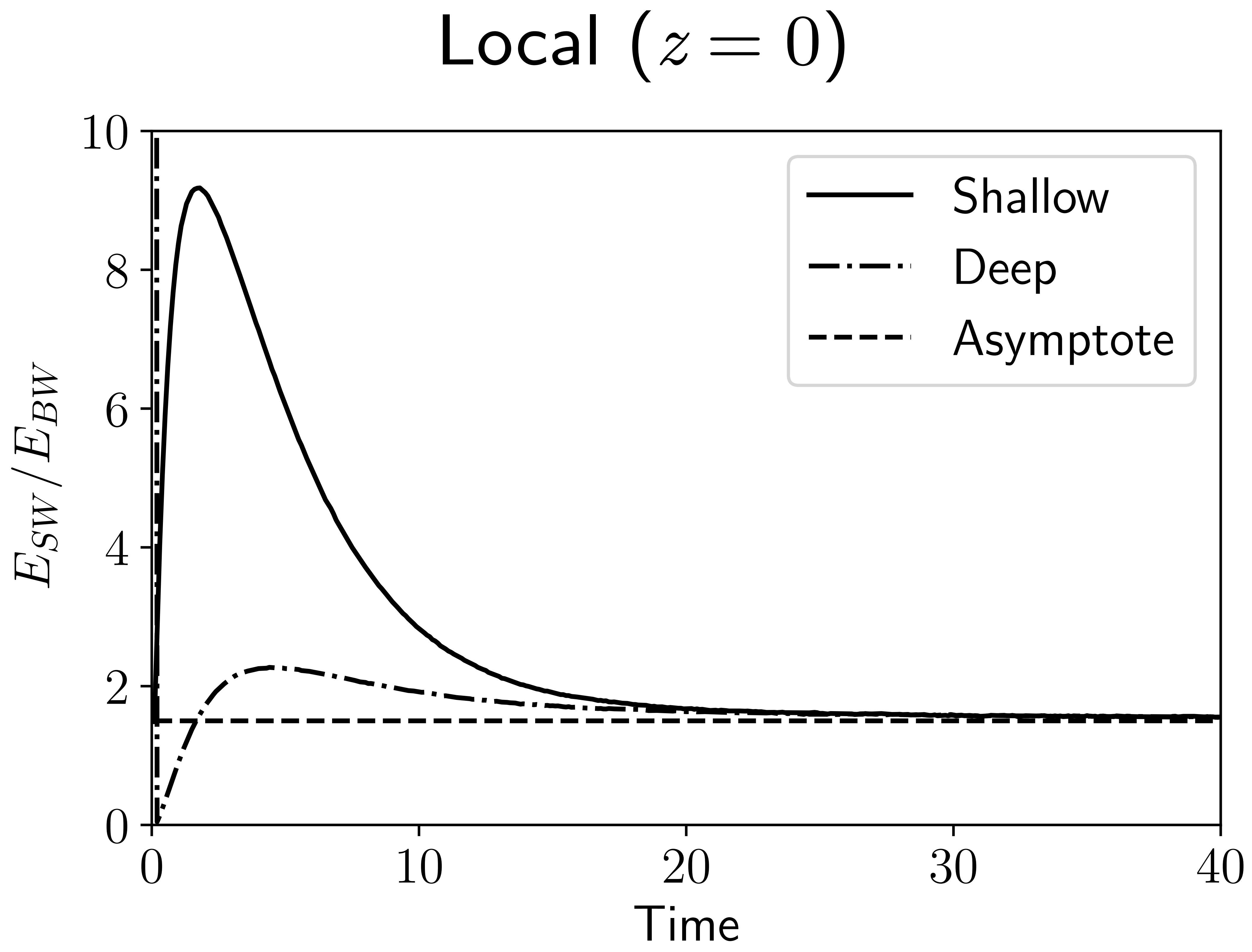

Energy Envelopes in Time Domain

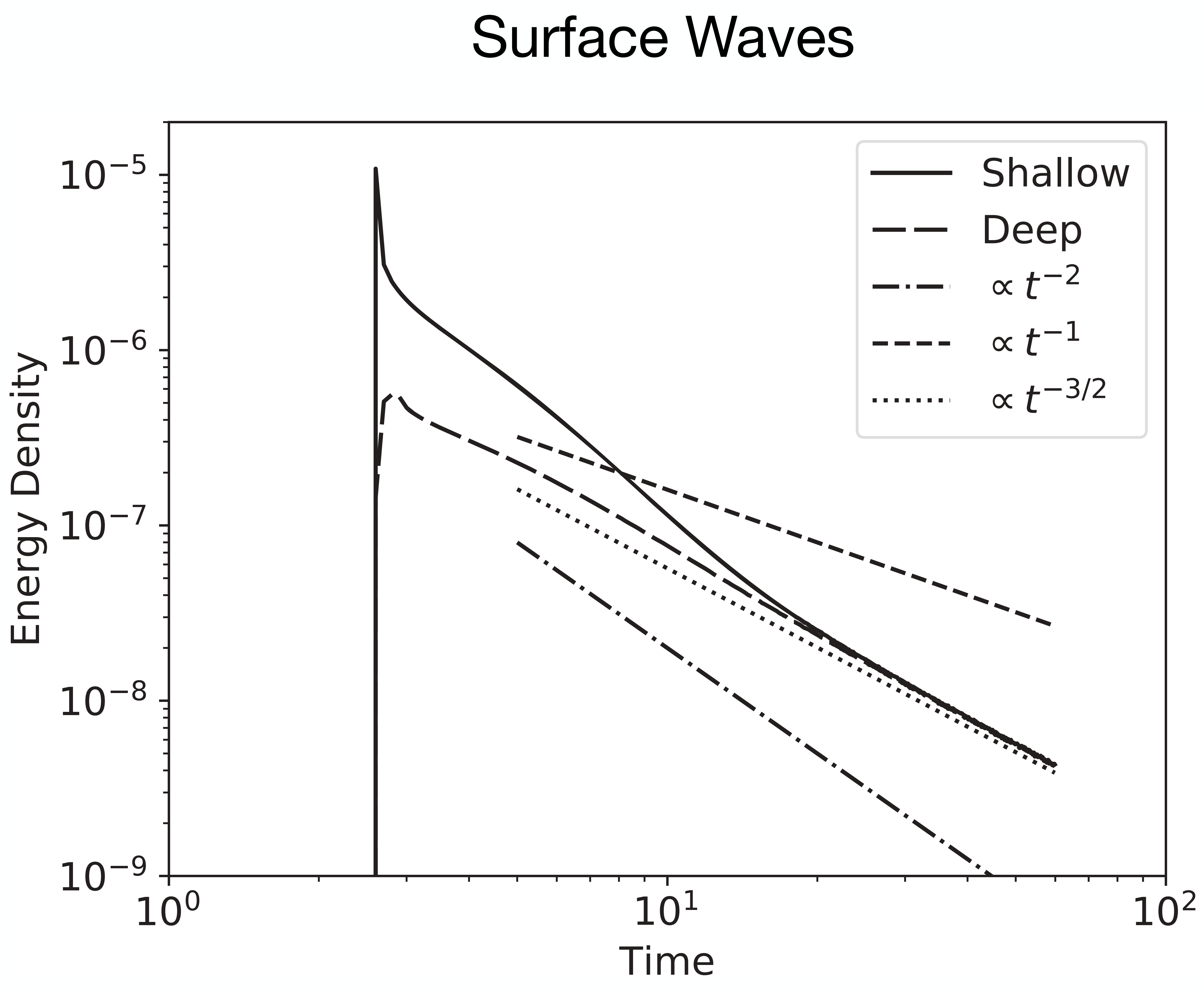

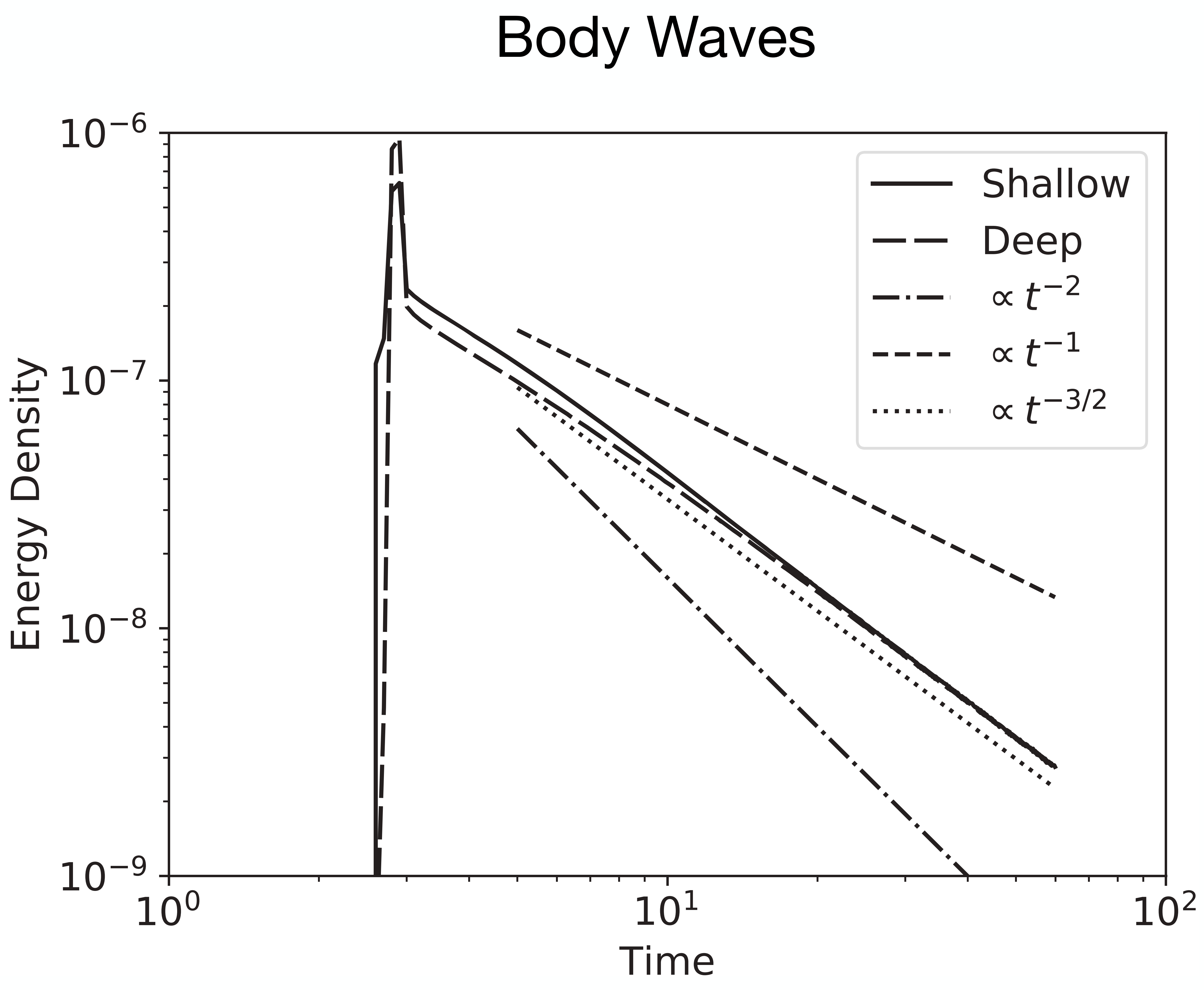

Delay Time Sensitivity Kernels

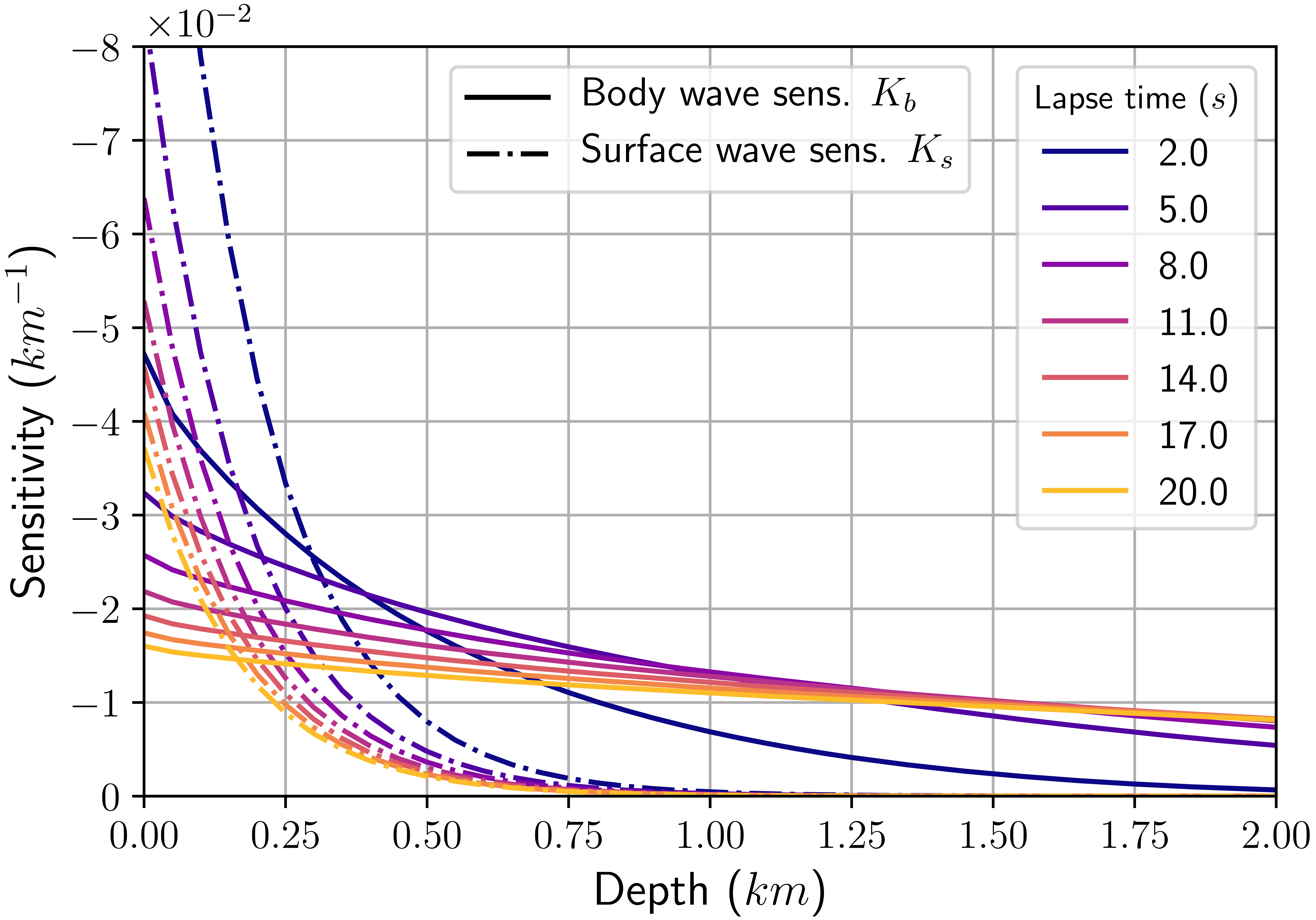

Barajas et al., 2022